Experiment Measurements of HyperNuclei Production from the High Baryon Density Region

Guannan Xie（谢冠男）

University of Chinese Academy of Sciences

April 15, 2024

Contents

- Introduction
- STAR Experiment & BES-II
- HyperNuclei Measurements @ STAR
  - ✓ Intrinsic Properties:
    -- Lifetime, Branch Ratios & Binding Energy
  - ✓ Productions and Collectivity:
    -- Centrality, Rapidity & Energy Dependence
- Summary and Outlook

Experimental Exploring of QCD Matters

Particle production:

- ➢ Understand medium properties and different particle production mechanisms

Collective flow:

- ➢ Study properties of the produced medium, EoS

Correlations and Criticality:

- ➢ Critical Point

……

Phys. Rev. Lett. 91 (2003) 72304

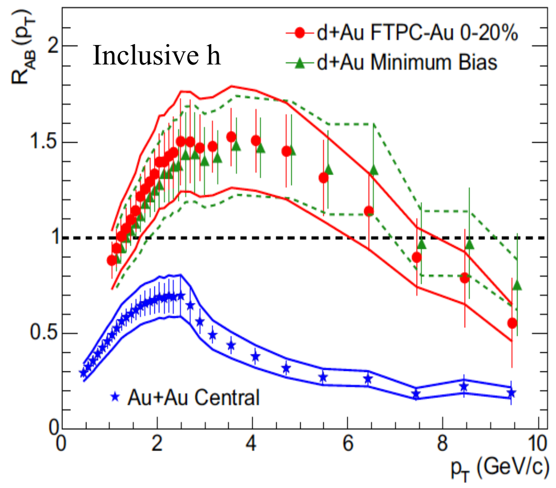

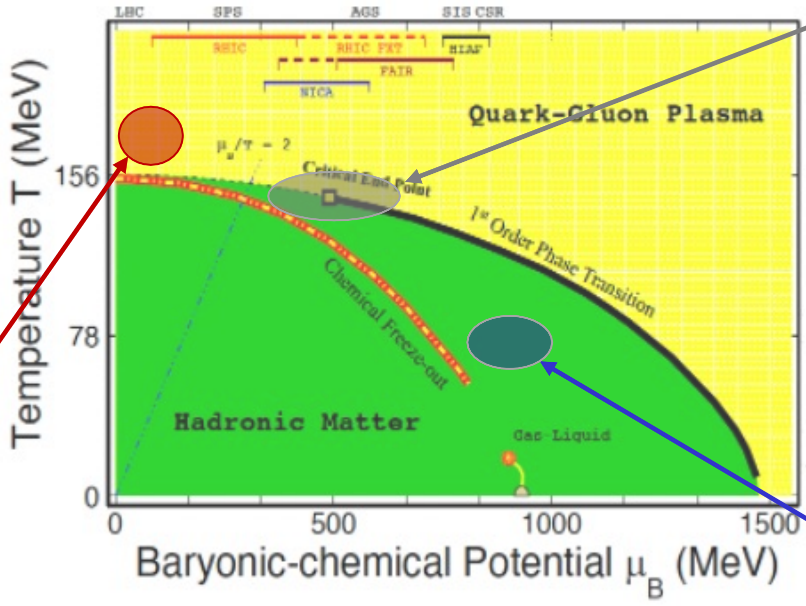

Phys. Rev. Lett. 128 (2022) 202303

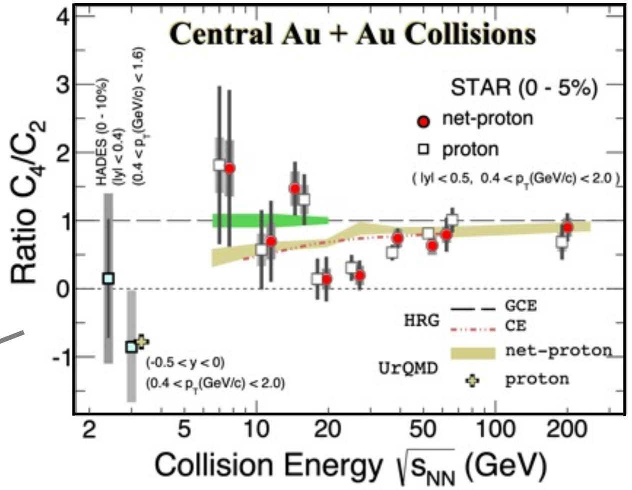

Phys. Lett. B 827 (2022) 137003

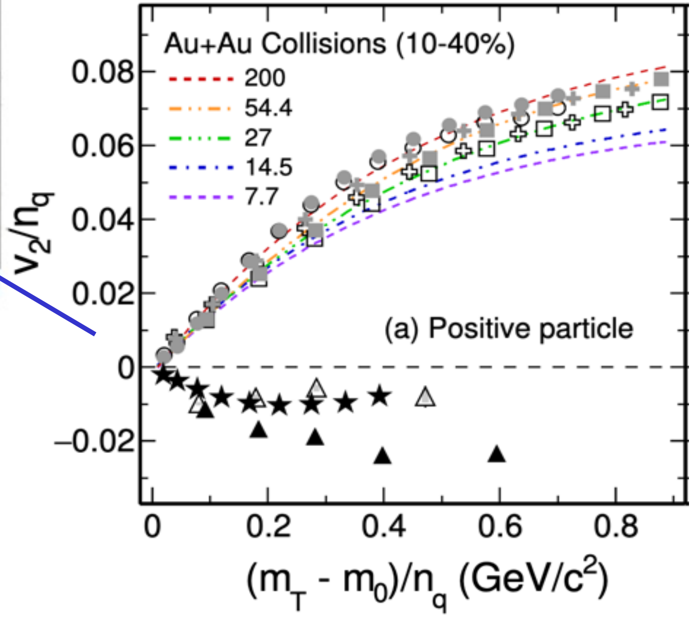

- Jet quenching, Strangeness enhancement, flow NCQ scaling, heavy flavor R_{AA}, etc
- High order Cumulants, light nuclei ratios
- NCQ disappearing, strangeness CE

Hypernuclei (What)

Nuclei are loosely bound objects with binding energies of few MeV
Hypernuclei are nuclei containing at least one hyperon (Y)
- N/Z + additional dimension on strangeness

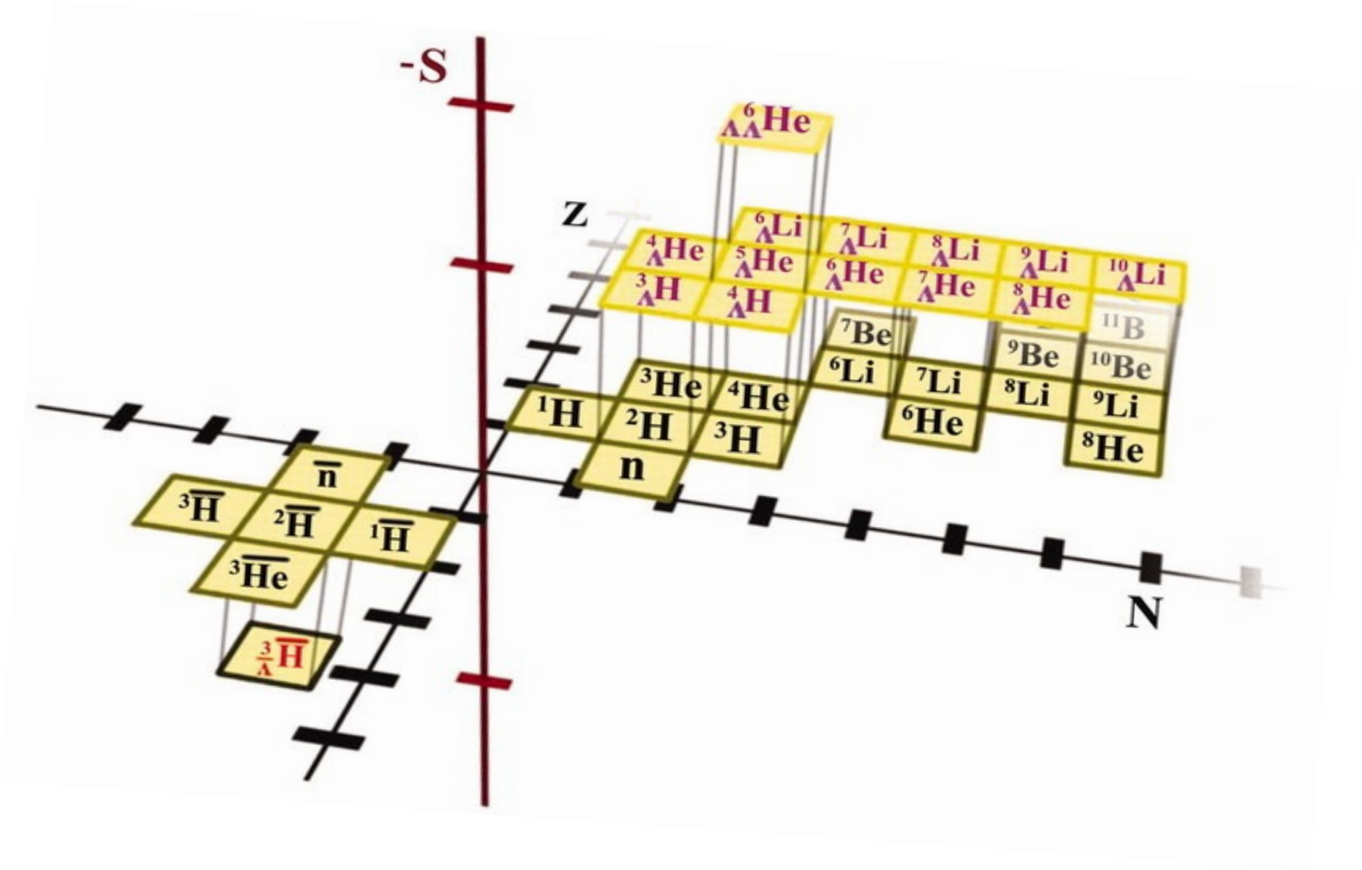

Figure from Science 328 (2010) 58-62

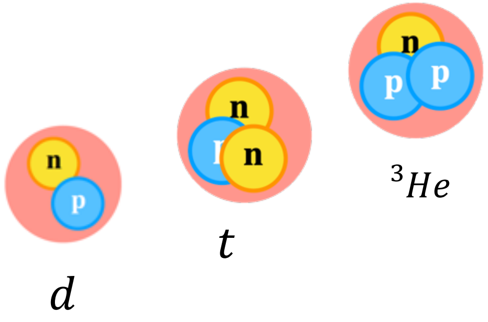

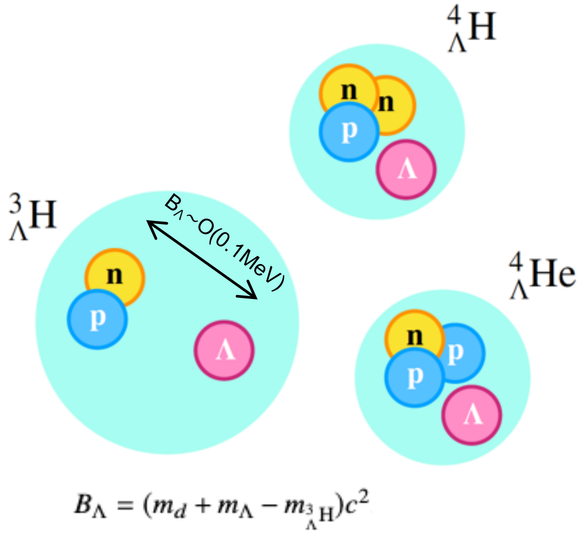

Phys. Lett. B 684 (2010) 224
Phys. Lett. B 781 (2018) 499
Phys.Rev. Lett. 114, 092301 (2015)

Hypernuclei (Why)

1. What can (hyper)nuclei production in heavy-ion collisions tell us about the QCD phase diagram and the nuclear equation-of-state?

- Sensitive to critical fluctuations and the onset of deconfinement

$$\frac{t \times p}{d^2}$$

Sensitive to neutron density fluctuations

$$\frac{{}^{3}_{\Lambda}\mathrm{H}}{{}^{3}\mathrm{He} \times \frac{\Lambda}{\mathrm{p}}}$$

Sensitive to baryon-strangeness correlations

2. What is the role of hyperon-nucleon (YN) and hyperon-hyperon (YY) interaction in the equation-of-state of high baryon density matter

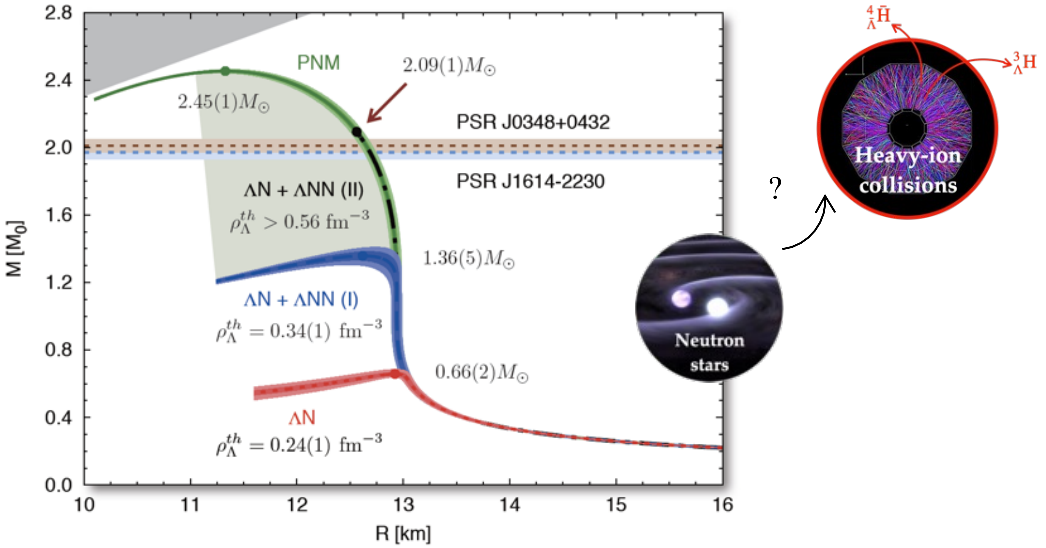

- Hyperon Puzzle: difficulty to reconcile the measured masses of neutron stars with the presence of hyperons in their interiors

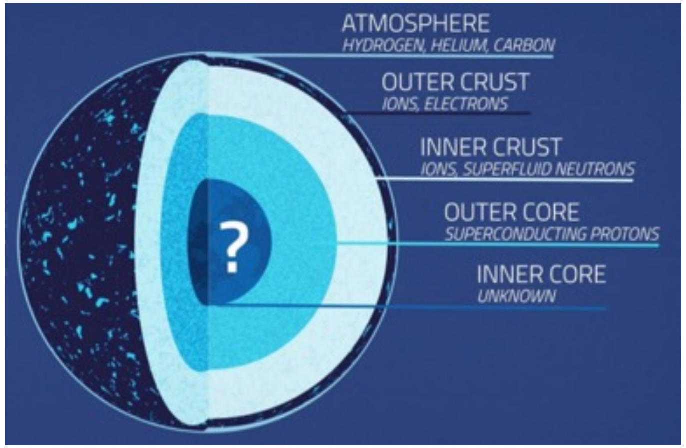

EoS governs the structure of neutron stars.

Hypernuclei (How)

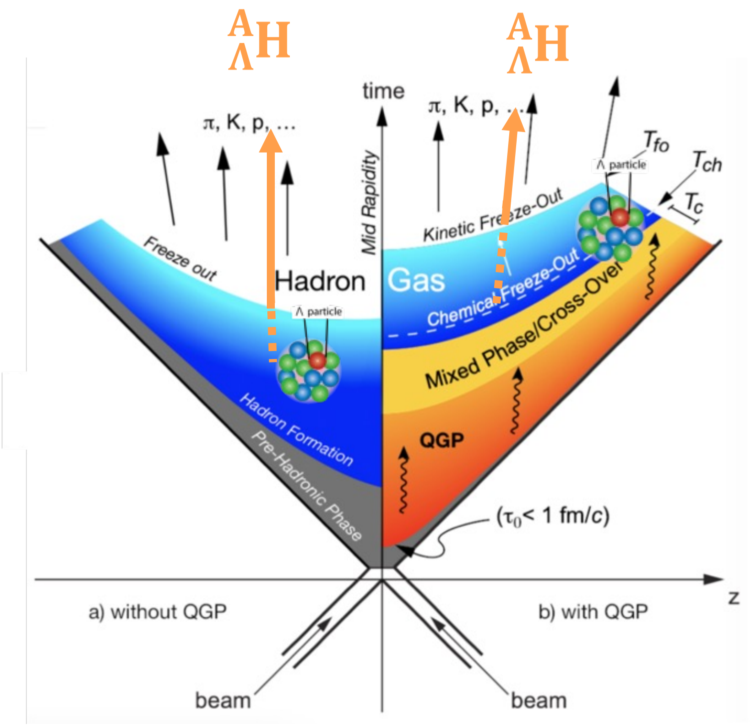

When are hypernuclei formed?
At freezeout? Or in medium?

1. Intrinsic properties: Internal structure
   - Lifetime, binding energy, branching ratio etc.

Understanding hypernuclei structure can provide insights to the Y-N interaction and EoS

2. Production mechanism
   - Spectra, Yields, Collectivity etc

The process of hypernuclei formation in violent heavy-ion collisions is not well understood

Hypernuclei production mechanism in HIC

Y. Ji. STAR, DNP 2023

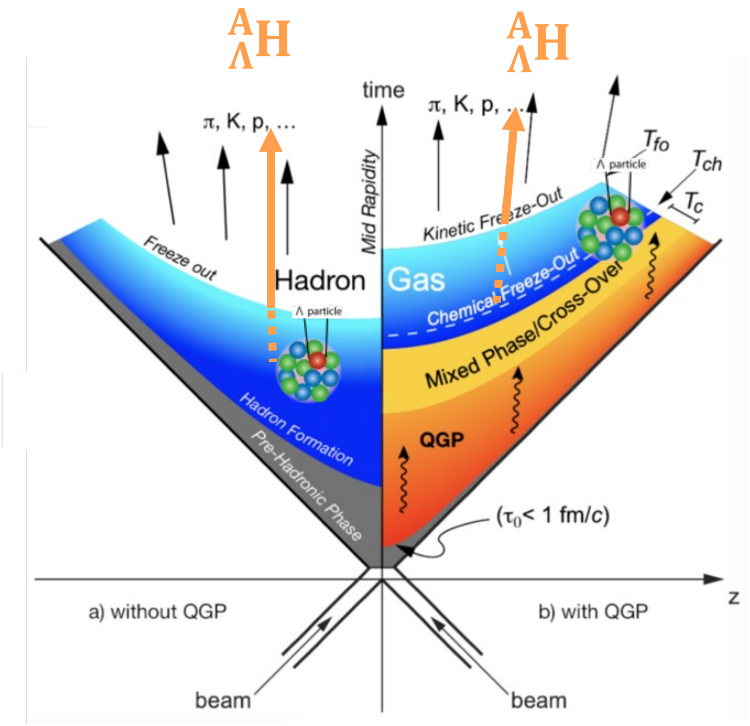

When and how are hypernuclei formed?
At freezeout? Or in medium?
Thermal or Coalescence?

$^{3}_{\Lambda}$H B_{Λ}~0.07-0.4 MeV, T_{ch}>>B_{Λ}

- Coalescence formation
  - Dominates at mid-rapidity
  Baryons / nuclei very close in phase space ($\vec{p}$, $\vec{r}$)
- Nuclear fragmentation of hypercluster
  - Dominates at beam rapidity
  Dominate for heavy hypernuclei formation
- Thermal model
  - Hadron chemical freeze out T_{ch} and μ_B
- Coalescence approach
  - Coalescence via final state interactions among nucleons
- Dynamical cluster formation
  - Reaction-based; clusters can be formed before kinetic freeze-out.

RHIC

Brookhaven National Laboratory (BNL), Upton, NY

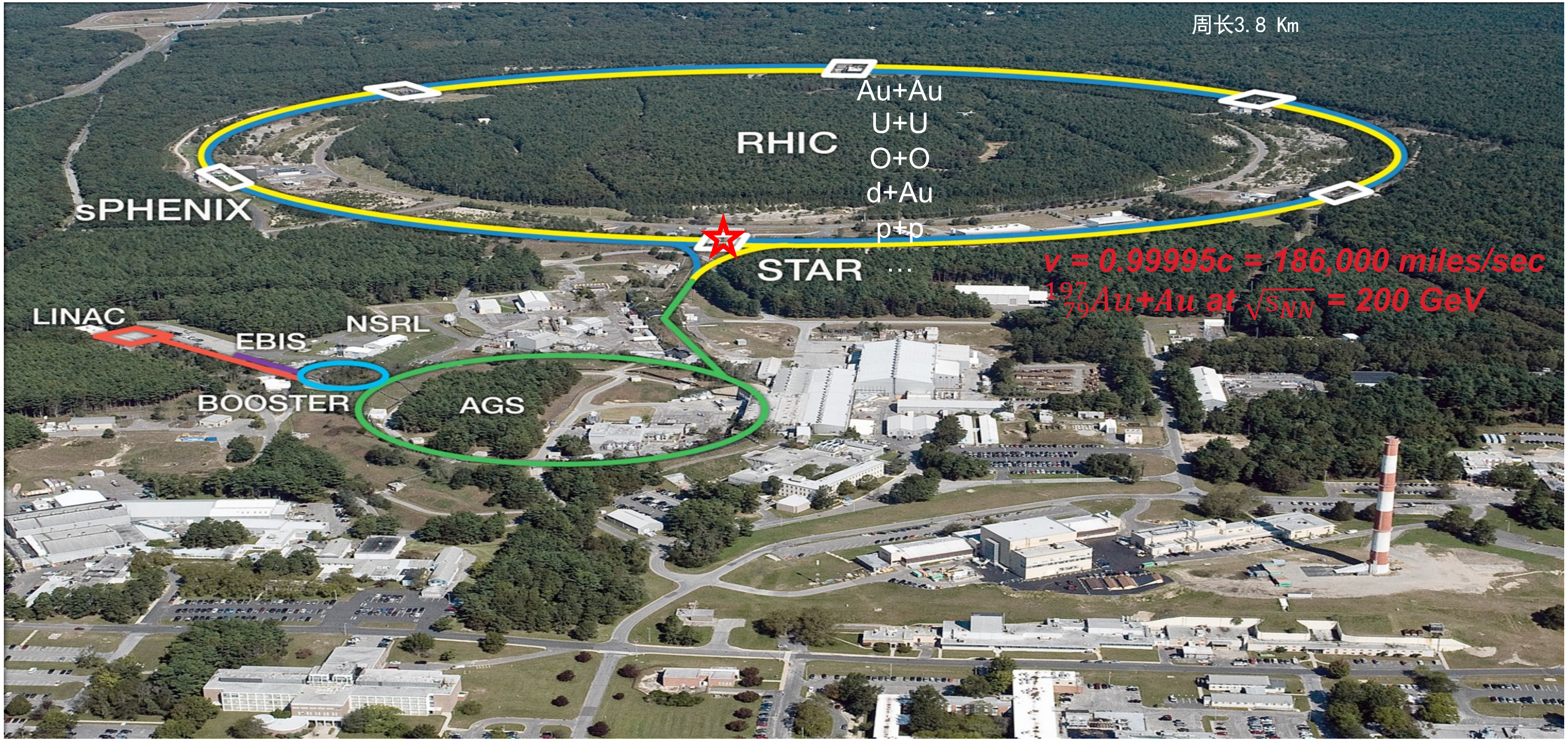

Relativistic **H**eavy **I**on **C**ollider

STAR Experimental

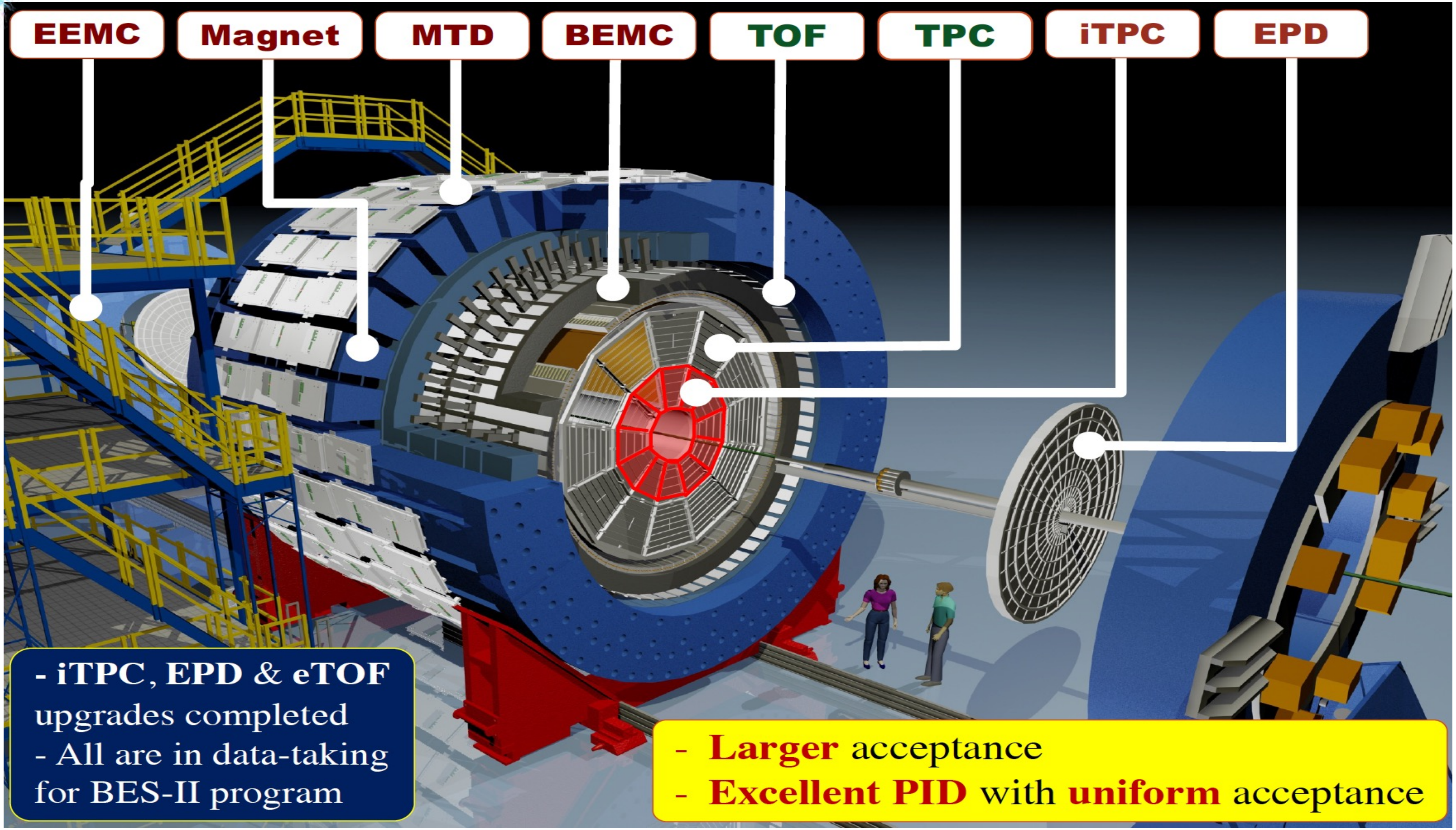

STAR Experimental & PID

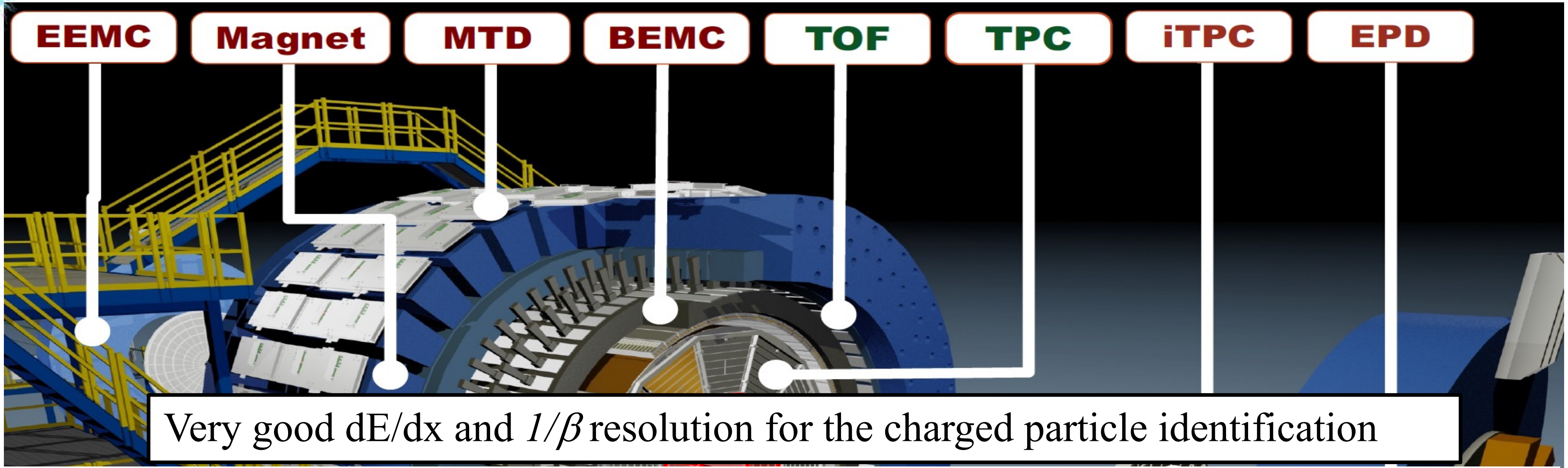

Very good dE/dx and *1/β* resolution for the charged particle identification

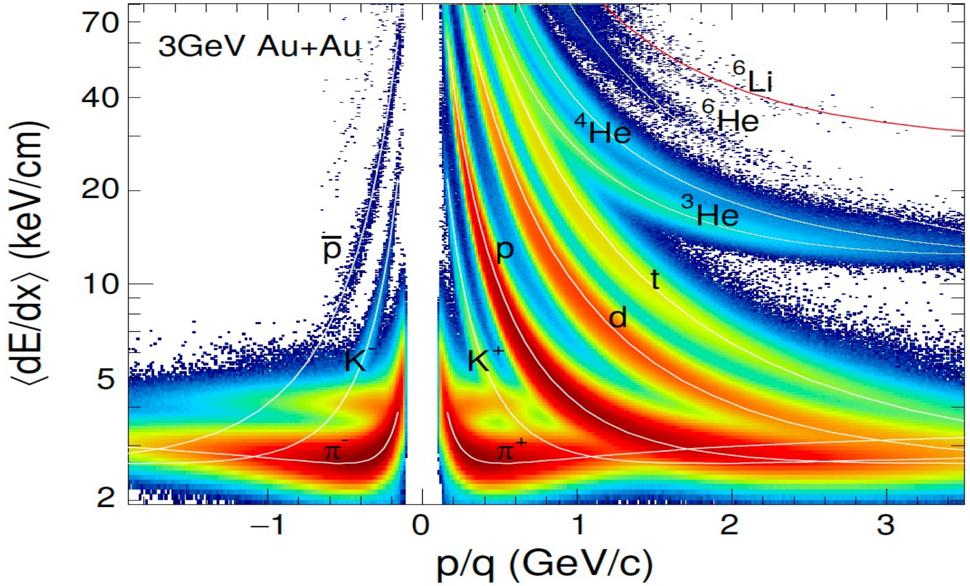

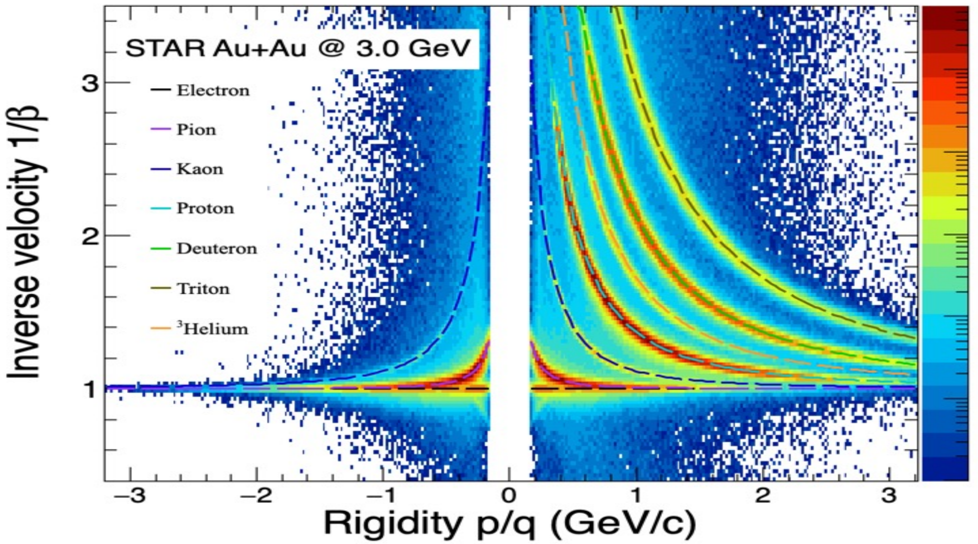

FXT Setup @ STAR

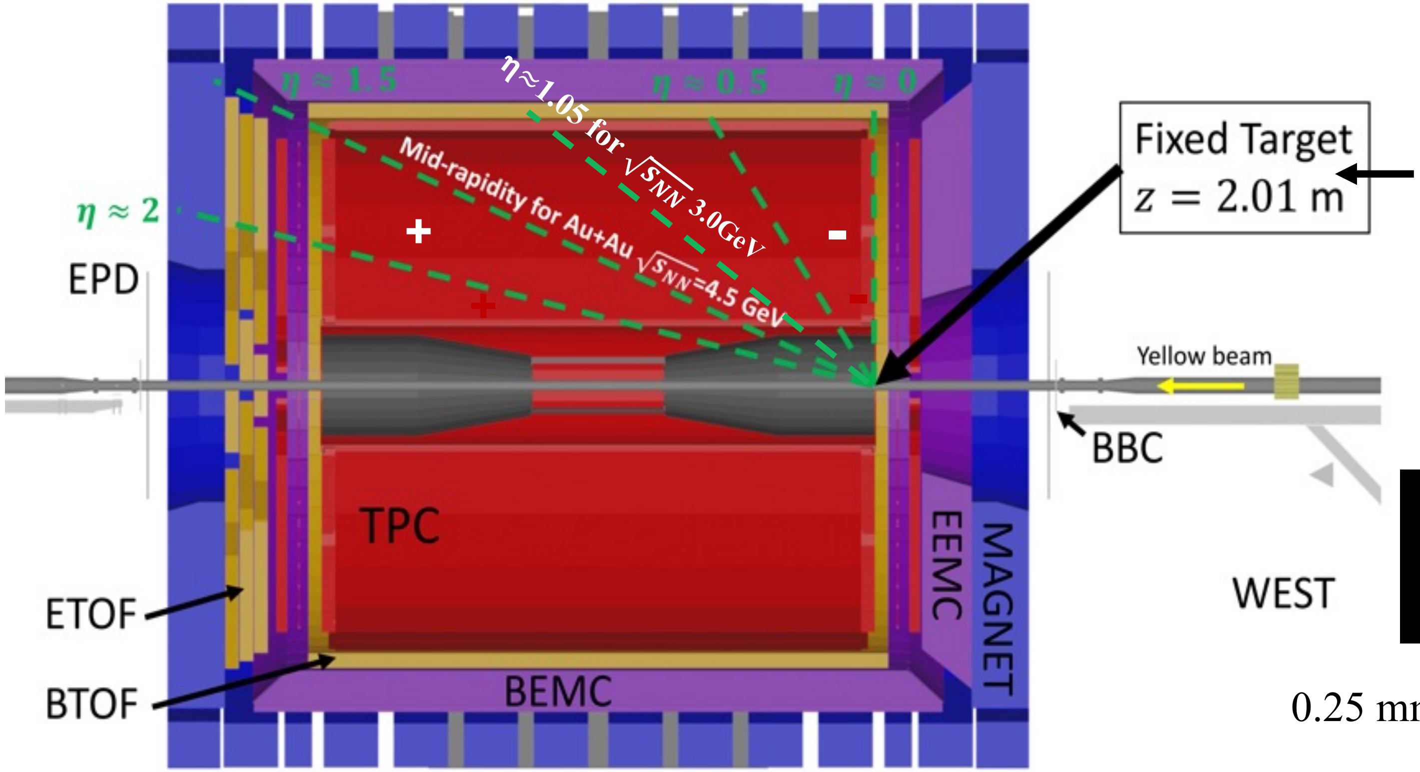

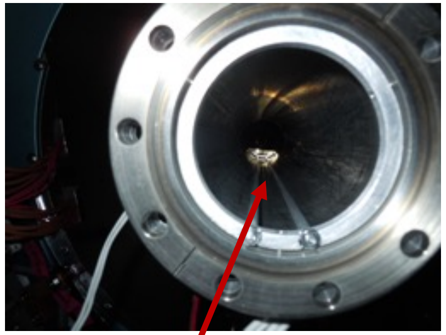

0.25 mm thickness Au-Target

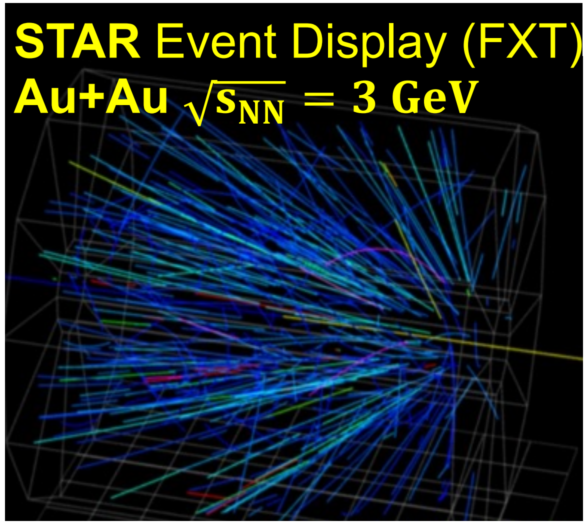

Good mid-rapidity coverage for STAR FXT 3 GeV (and up to 4.5GeV)

Conventions: beam-going direction is the positive direction

STAR Beam Energy Scan

Au+Au Collisions at RHIC											
Collider Runs						Fixed-Target Runs					
	$\sqrt{s_{NN}}$ (GeV)	#Events	μ_B	y_{beam}	run		$\sqrt{s_{NN}}$ (GeV)	#Events	μ_B	y_{beam}	run
1	200	380M	25MeV	5.3	r10,19	1	13.7(100)	50M	280MeV	-2.69	r21
2	62.4	46M	75MeV		r10	2	11.5(70)	50M	320MeV	-2.51	r21
3	54.4	1200M	85MeV		r17	3	9.2(44.5)	50M	370MeV	-2.28	r21
4	39	86M	112MeV		r10	4	7.7(31.2)	260M	420MeV	-2.1	r18,19,20
5	27	585M	156MeV	3.36	r11,18	5	7.2(26.5)	470M	440MeV	-2.02	r18,20
6	19.6	595M	206MeV	3.1	r11,19	6	6.2(19.5)	120M	490MeV	-1.87	r20
7	17.3	256M	230MeV		r21	7	5.2(13.5)	100M	540MeV	-1.68	r20
8	14.6	340M	262MeV		r14,19	8	4.5(9.8)	110M	590MeV	-1.52	r20
9	11.5	57M	316MeV		r10,20	9	3.9(7.3)	120M	633MeV	-1.37	r20
10	9.2	160M	372MeV		r10,20	10	3.5(5.75)	120M	670MeV	-1.2	r20
11	7.7	104M	420MeV		r21	11	3.2(4.59)	200M	699MeV	-1.13	r19
						12	3.0(3.85)	260+ 2000M	760MeV	-1.05	r18,20

Most Precise data to map the QCD phase diagram, $3 < \sqrt{s_{NN}} < 200\ GeV; 760 > \mu_B > 25\ MeV;$

Hypernuclei in HIC at High Baryon Density

Why heavy-ion collisions (HIC)?

- produced in copious amounts in HIC
- Potential for high precision measurements

- Collider mode：$\sqrt{s_{NN}}$ = 7.7 - 54GeV
- Fixed-Target mode：$\sqrt{s_{NN}}$ = 3.0 - 13.7GeV

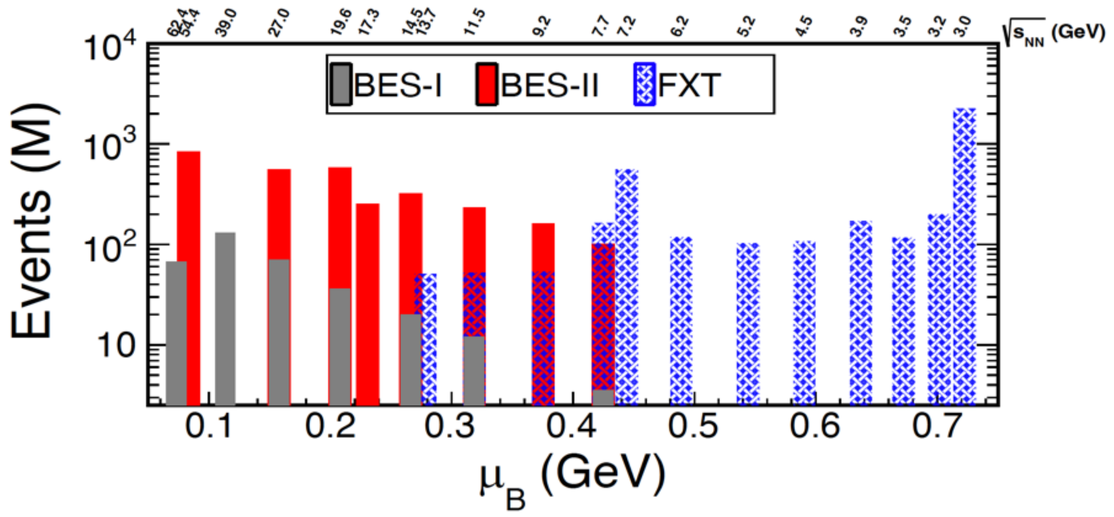

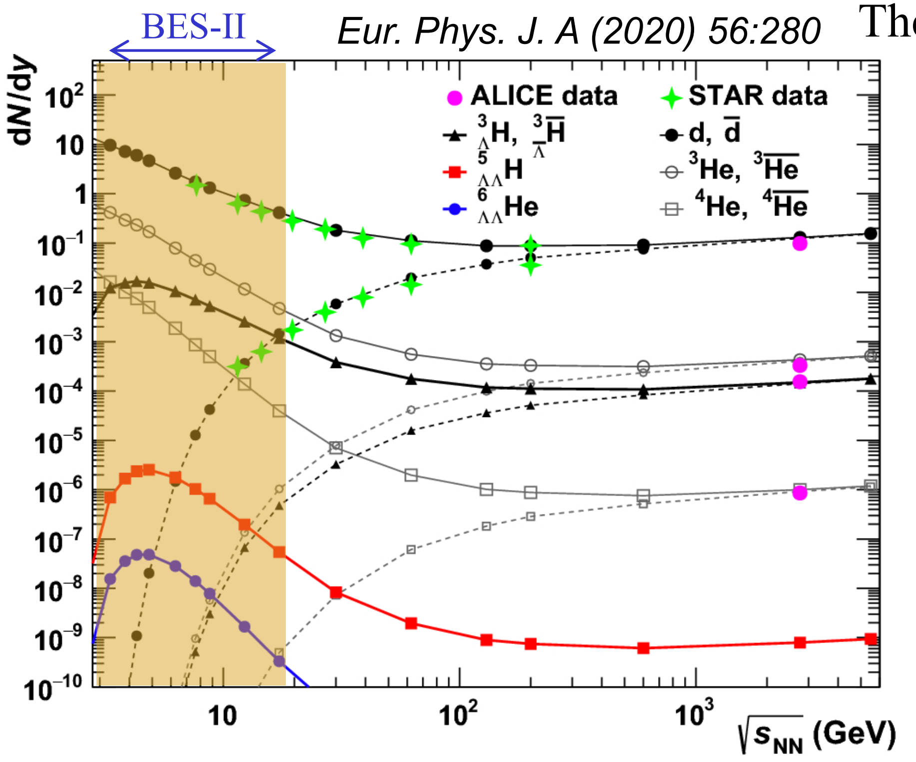

- Productions mechanism
  - thermal, coalescence, fragmentation
- Intrinsic properties
  - cτ, *BR.*, B_Λ

- Recently released hypertriton results from 3.2, 3.5, 3.9, 4.5,7.7,14.6 GeV

Hypernuclei Signal Reconstruction

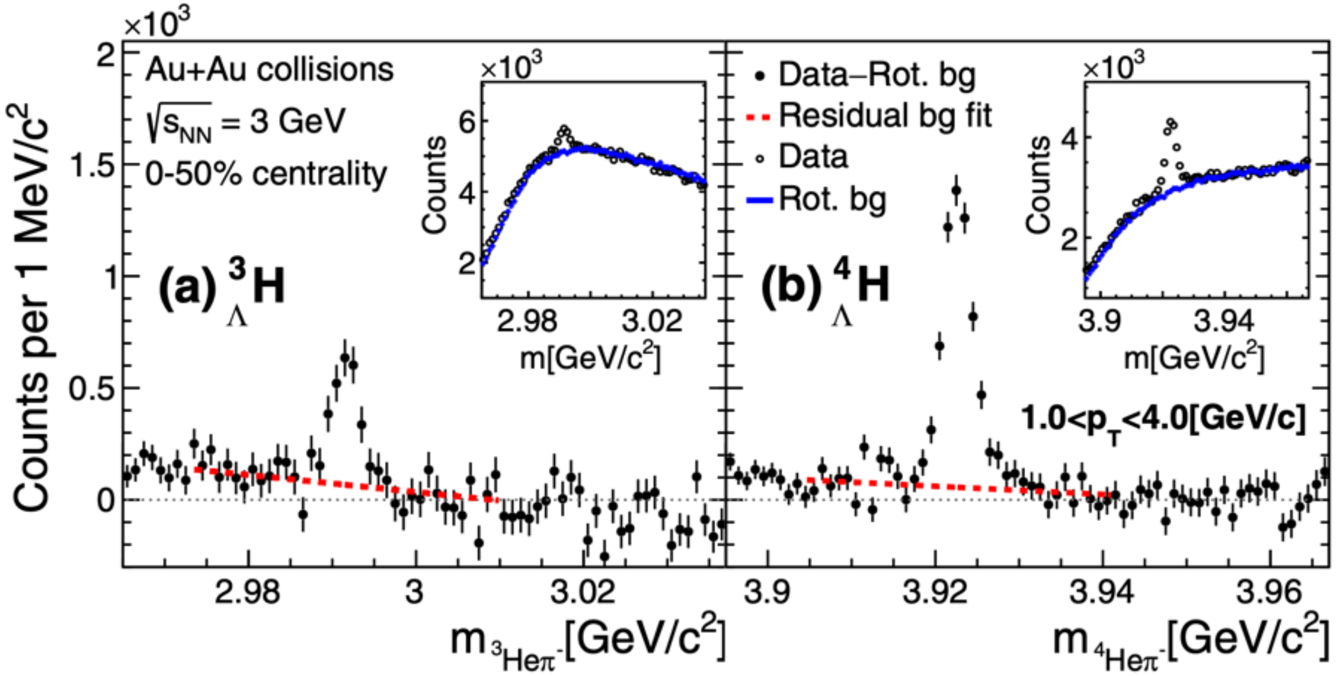

Phys. Rev. Lett. 128 (2022) 20, 202301
Y. Ji. Y Leung, STAR, QM 2023

New hypertriton results from
3.2, 3.5, 3.9, 4.5 GeV (FXT)
7.7,14.6 GeV (COL)

$$^{3}_{\Lambda}H \rightarrow {}^{3}He\,\pi^- \,;\; ^{4}_{\Lambda}H \rightarrow {}^{4}He\,\pi^-$$
$$^{3}_{\Lambda}H \rightarrow p\,d\,\pi^+ \,;\; ^{4}_{\Lambda}He \rightarrow {}^{3}He\,p\,\pi^+$$

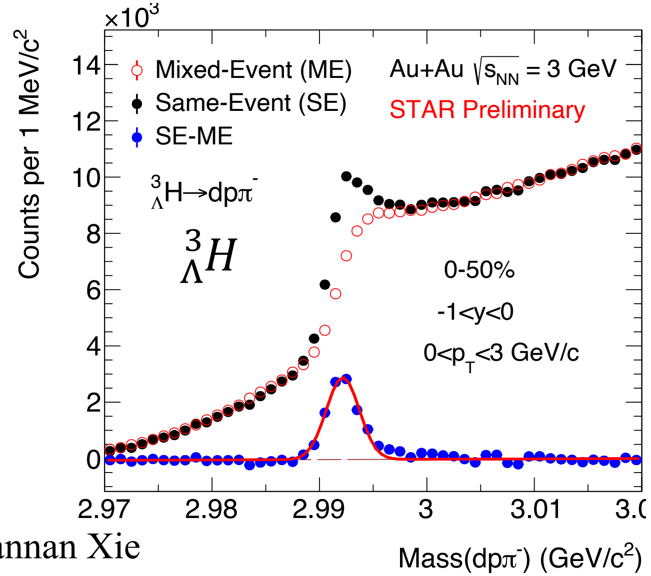

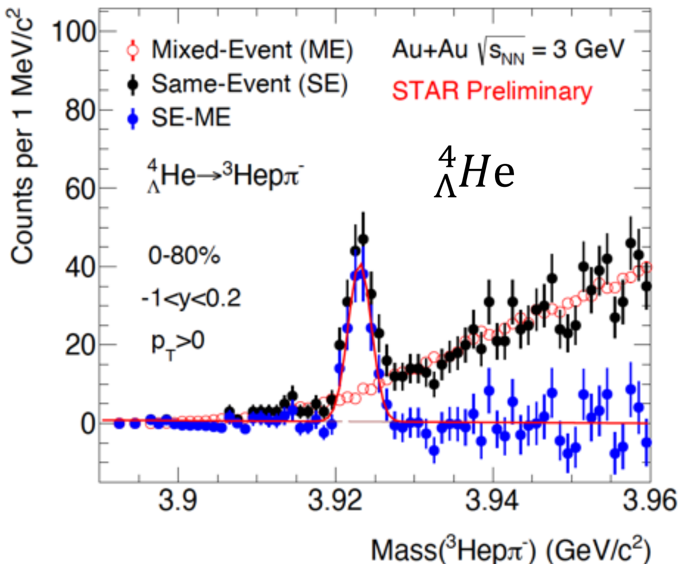

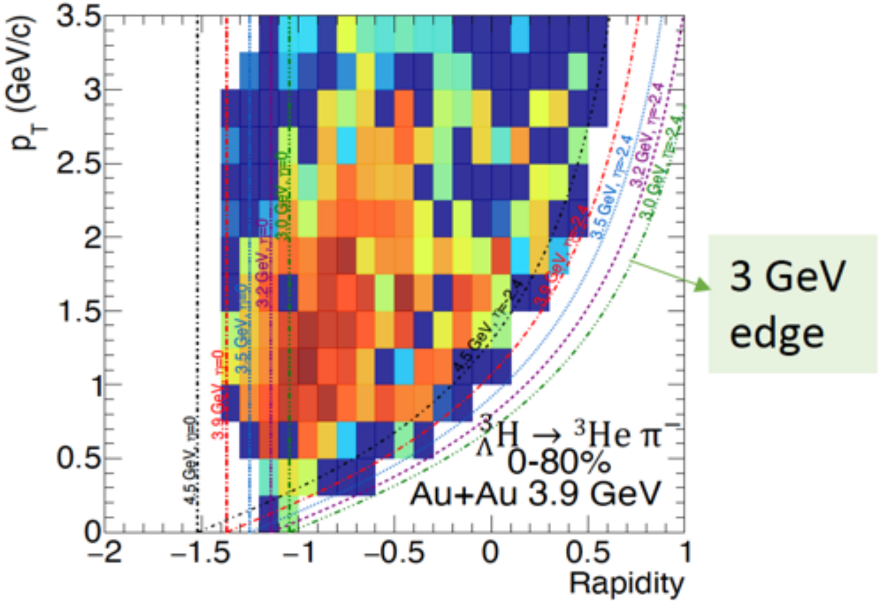

Hypernuclei Lifetime

- Light hypernuclei structure serves for our understanding of the YN interaction

Phys. Rev. Lett. 128 (2022) 20, 202301 *Lifetime*

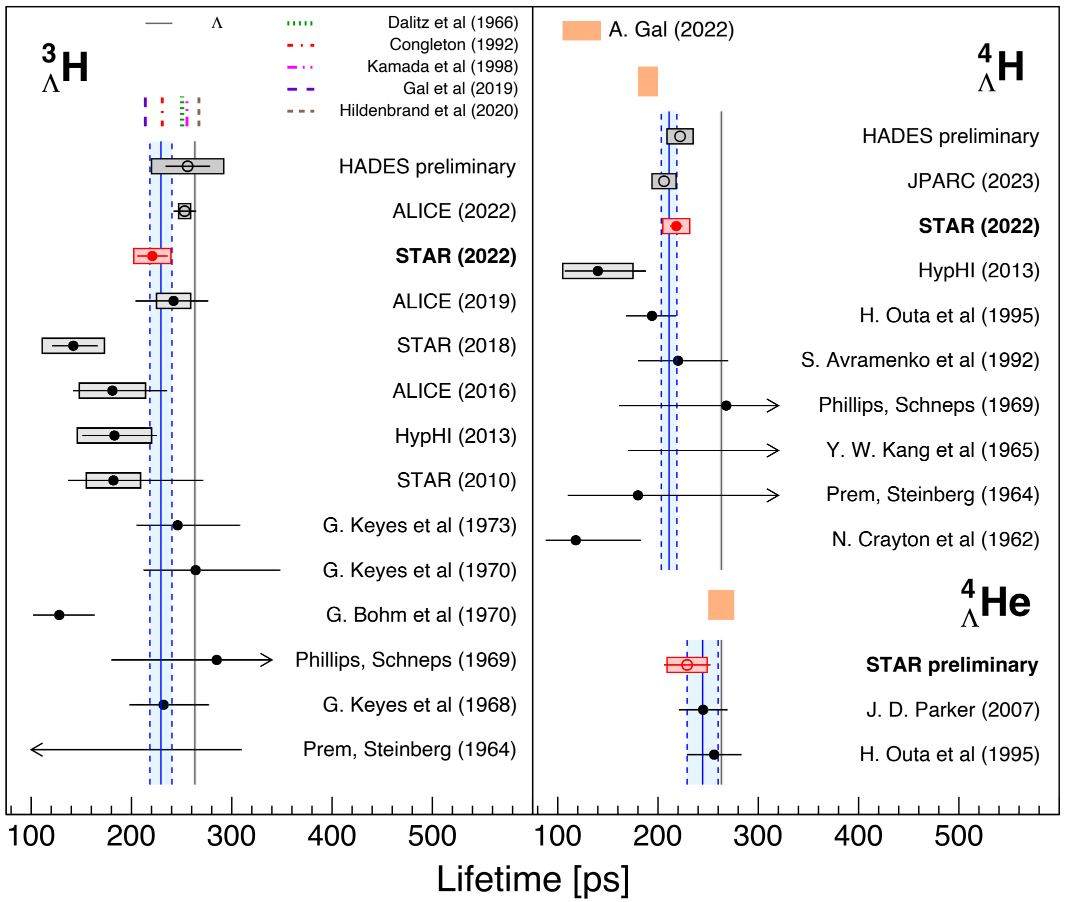

$$N(\tau) = N_0 e^{-L/\beta\gamma c\tau}$$

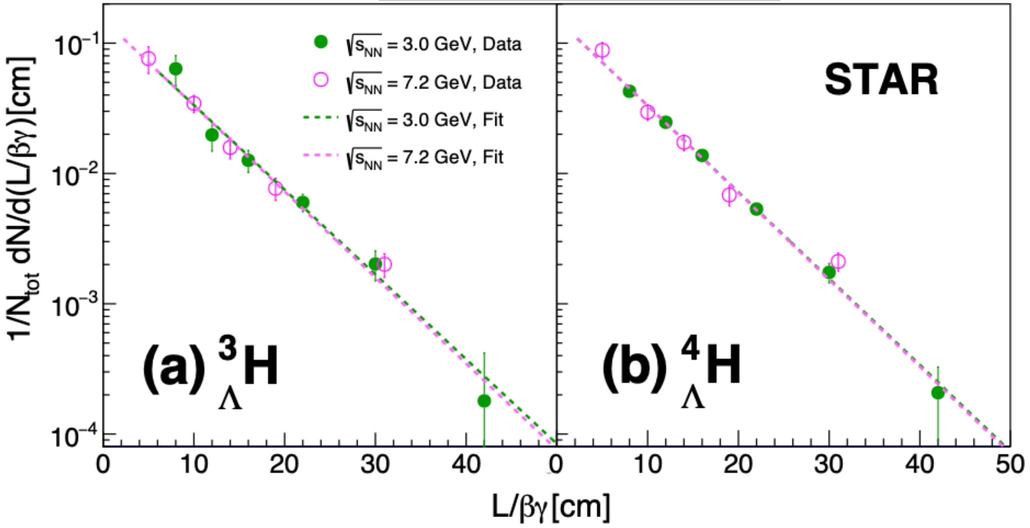

- Lifetime extracted from the exponential fit to the $\frac{dN}{d(L/\beta\gamma)}$

$^{3}_{\Lambda}$H: Global avg. = $(87\pm5)\%\tau(\Lambda)$, $2.8\sigma < \tau(\Lambda)$.

- Calculations with pion FSI consistent with data.

$^{4}_{\Lambda}$H, $^{4}_{\Lambda}$He: $\tau(^{4}_{\Lambda}\text{H})/\tau(^{4}_{\Lambda}He) = 0.86\pm0.06$.

- Lifetime ratio consistent with calculation based on isospin rule.

$$\frac{\Gamma(^{4}_{\Lambda}\text{He} \to {}^{4}\text{He} + \pi^0)}{\Gamma(^{4}_{\Lambda}\text{H} \to {}^{4}\text{He} + \pi^-)} \approx \frac{1}{2}$$

A. Gal, EPJ Web Conf. 259, 08002 (2022)

A. Gal et al, PLB791, 48 (2019)

ALICE, arXiv:2209.07360v2 ; HADES, S. Spies QM2022 ; JPARC, arXiv: 2302.07443

Hypernuclei @ 3GeV

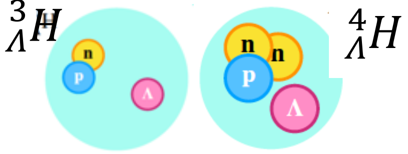

Phys. Rev. Lett. 128 (2022) 20, 202301

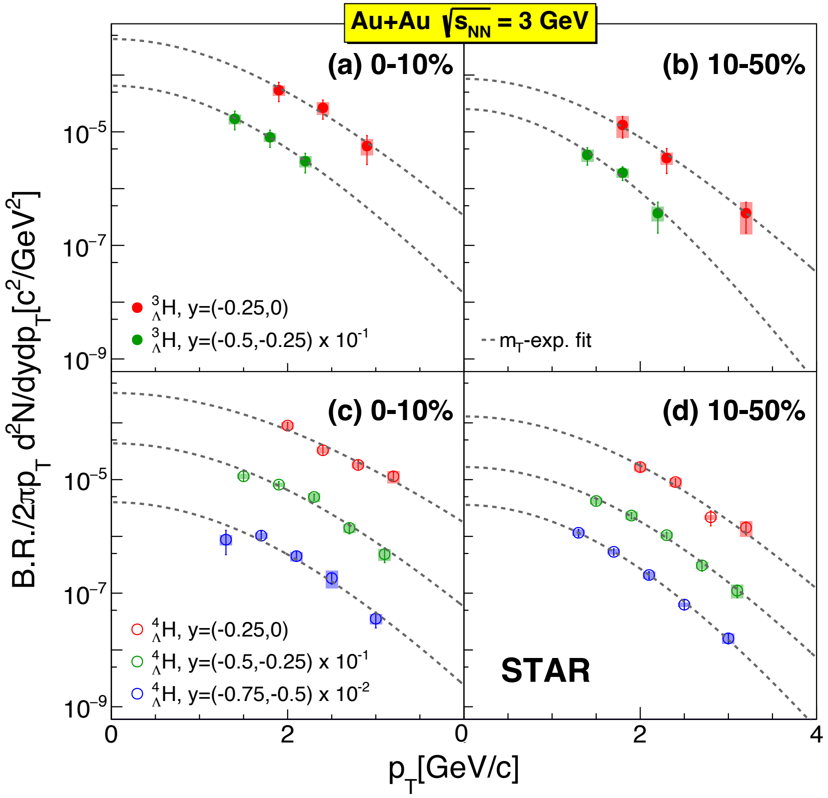

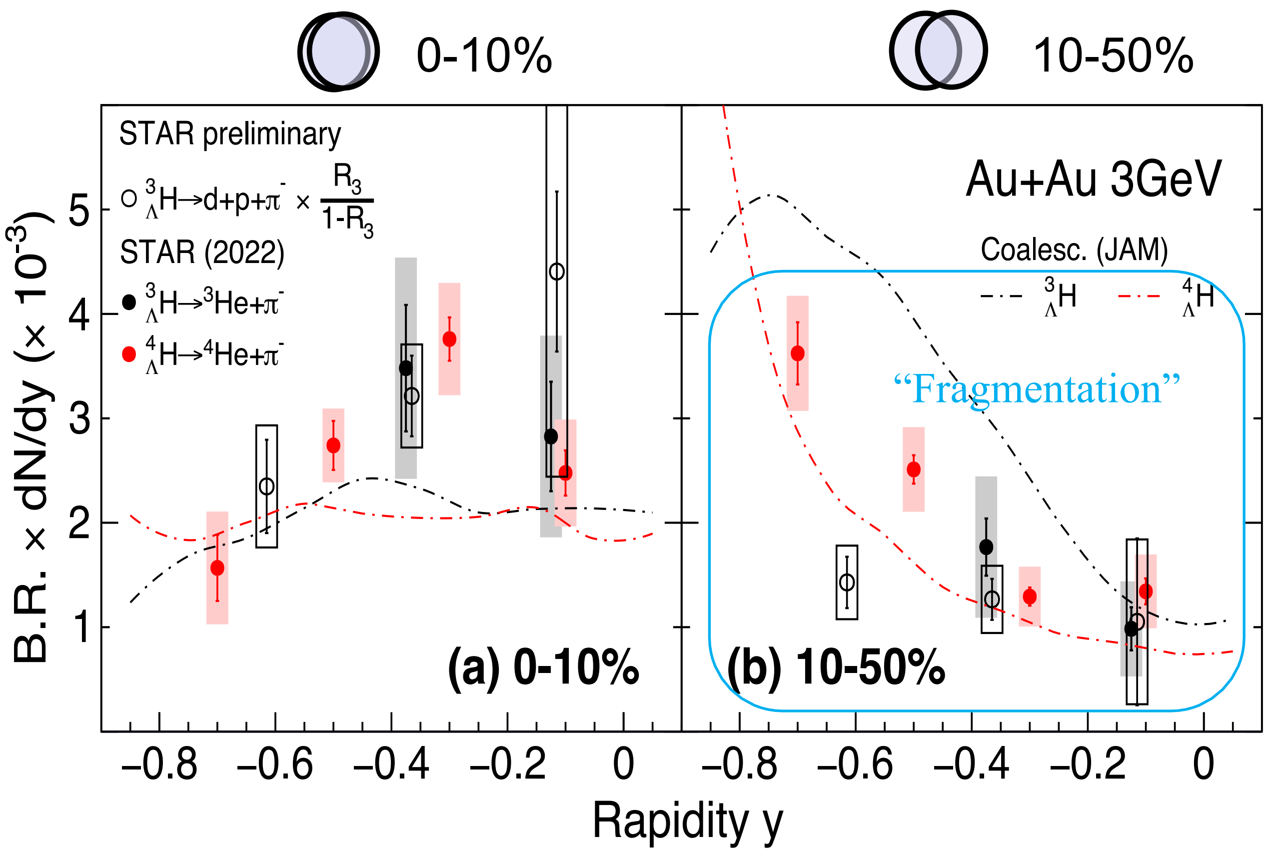

First measurements on rapidity dependence of hypernuclei yields in heavy ion collisions, consist b/w 2 body and 3 body.

Different trends in rapidity in 10-40% centrality regions. -> Fragmentation contribution

Transport model (JAM) with coalescence afterburner qualitatively reproduce trends of the rapidity distributions

Hypernuclei from BES-II Energies

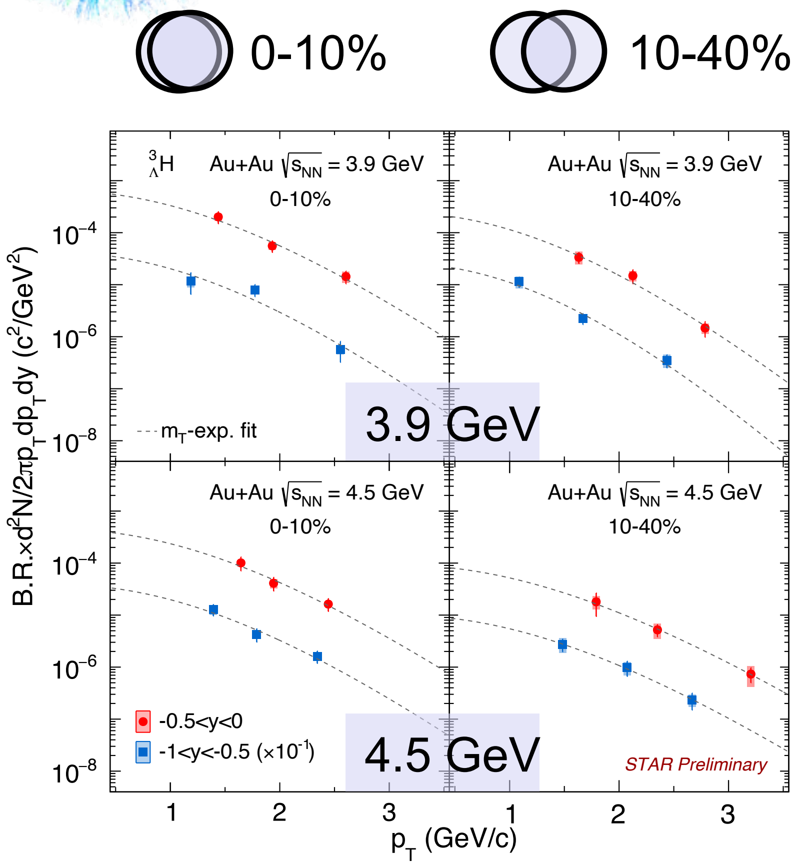

New $^{3}_{\Lambda}$H results @ 3.2, 3.5, 3.9, 4.5, from Y. Ji. etc @ 7.7 14.6GeV (Coll.) from Y Leung QM2023

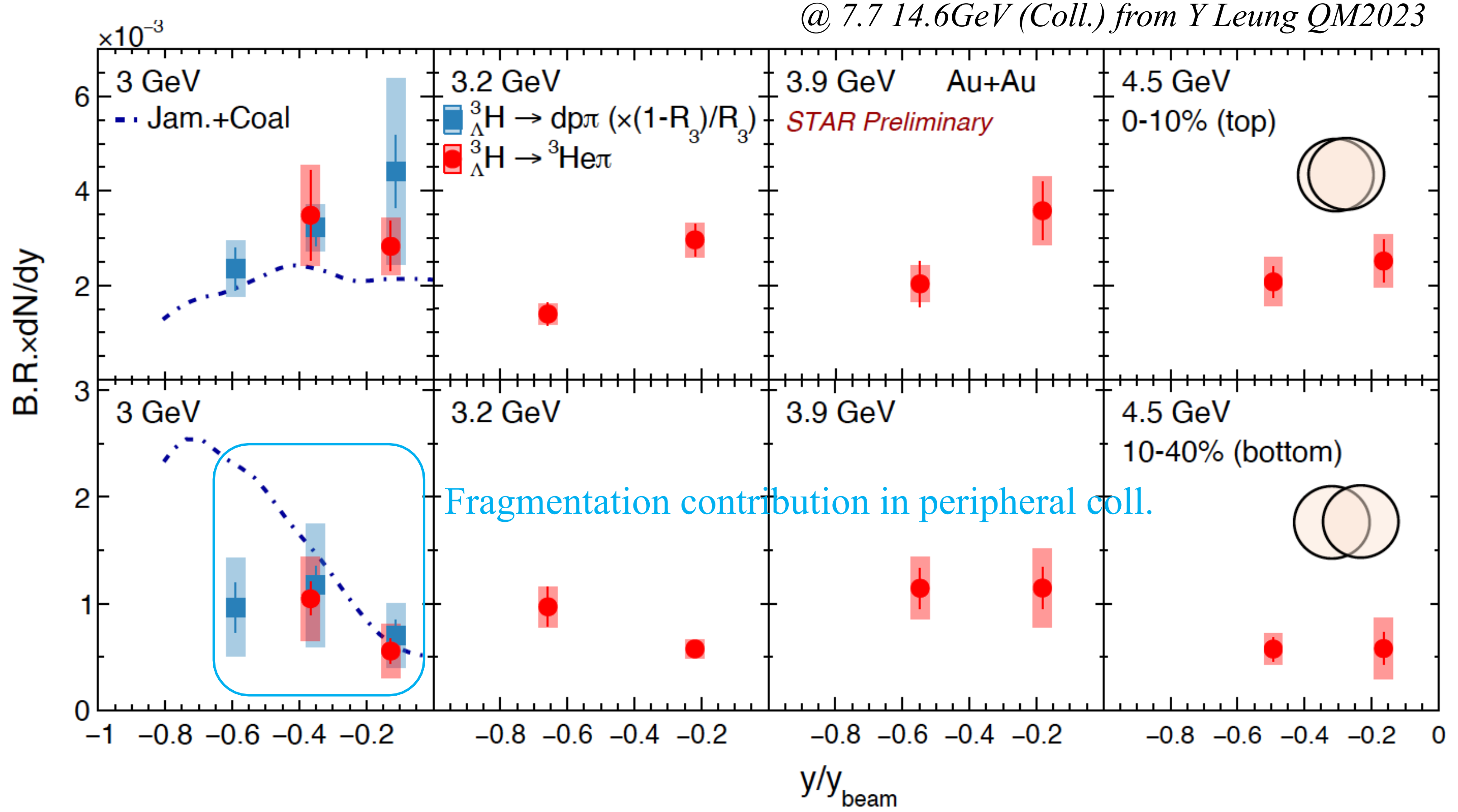

Utilizing datasets collected by STAR Fixed-Target program, $^{3}_{\Lambda}$H p_T spectra, dN/dy are measured at $\sqrt{(s_{NN})}$= 3-4.5 GeV in Au+Au collisions.

Also new released results from BES-II Collide mode @ 7.7 and 14.6 GeV

Hypernuclei Yield vs. $\sqrt{s_{NN}}$

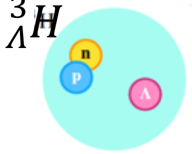

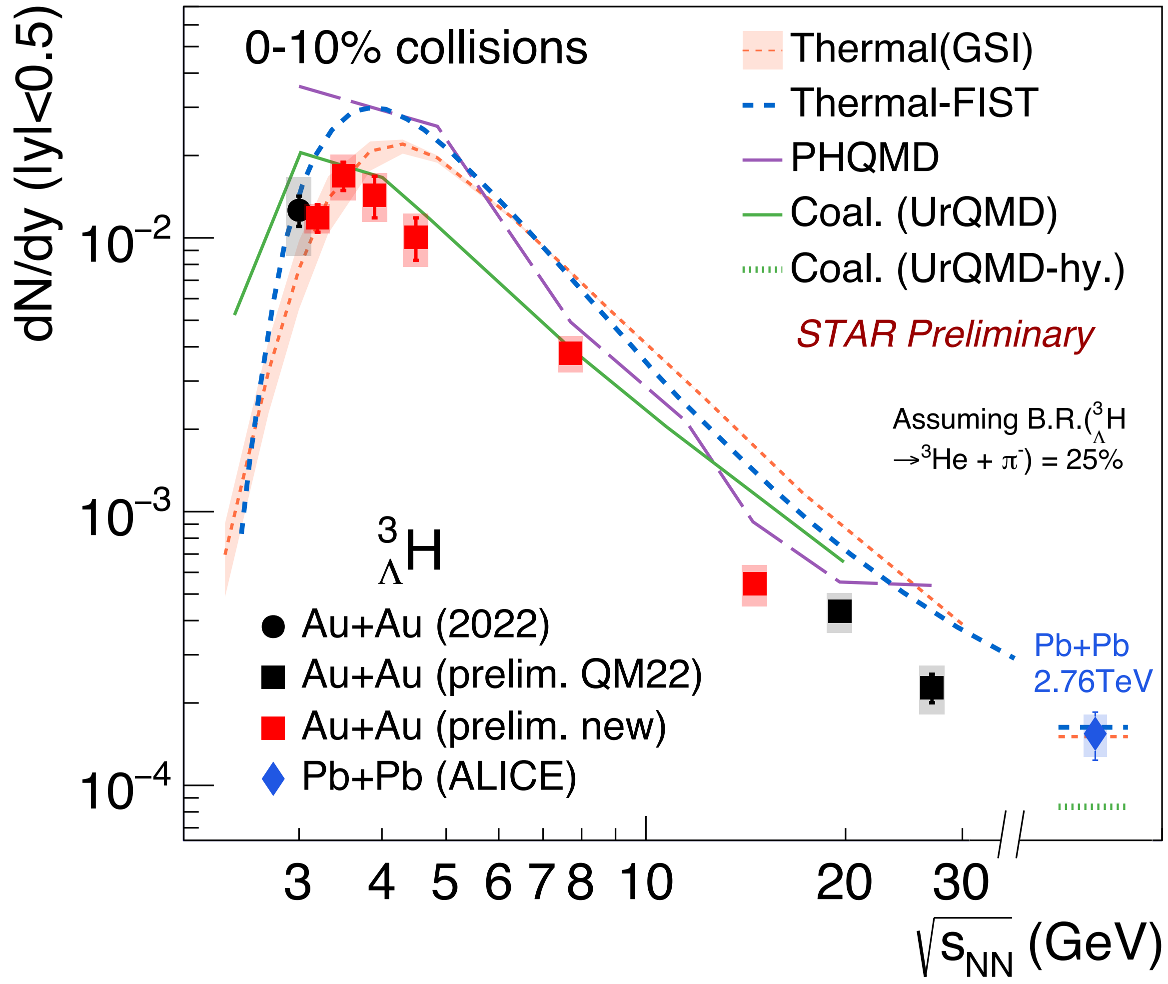

Pb+Pb: ALICE, PLB 754, 360 (2016)
STAR at 3 GeV: PRL 128, 202301 (2022)

First energy dependence of $^{3}_{\Lambda}H$ hypernuclei production yields in high baryon region

$^{3}_{\Lambda}H$ yields peak at $\sqrt{(s_{NN})}$ = 3-4 GeV then decrease toward higher energy

- Increasing baryon density at lower energies
- Stronger strangeness canonical suppression at low energies

Low Energies 3-4GeV optimal range search for $\Lambda\Lambda$-hypernuclei

Hypernuclei Yield vs. $\sqrt{s_{NN}}$

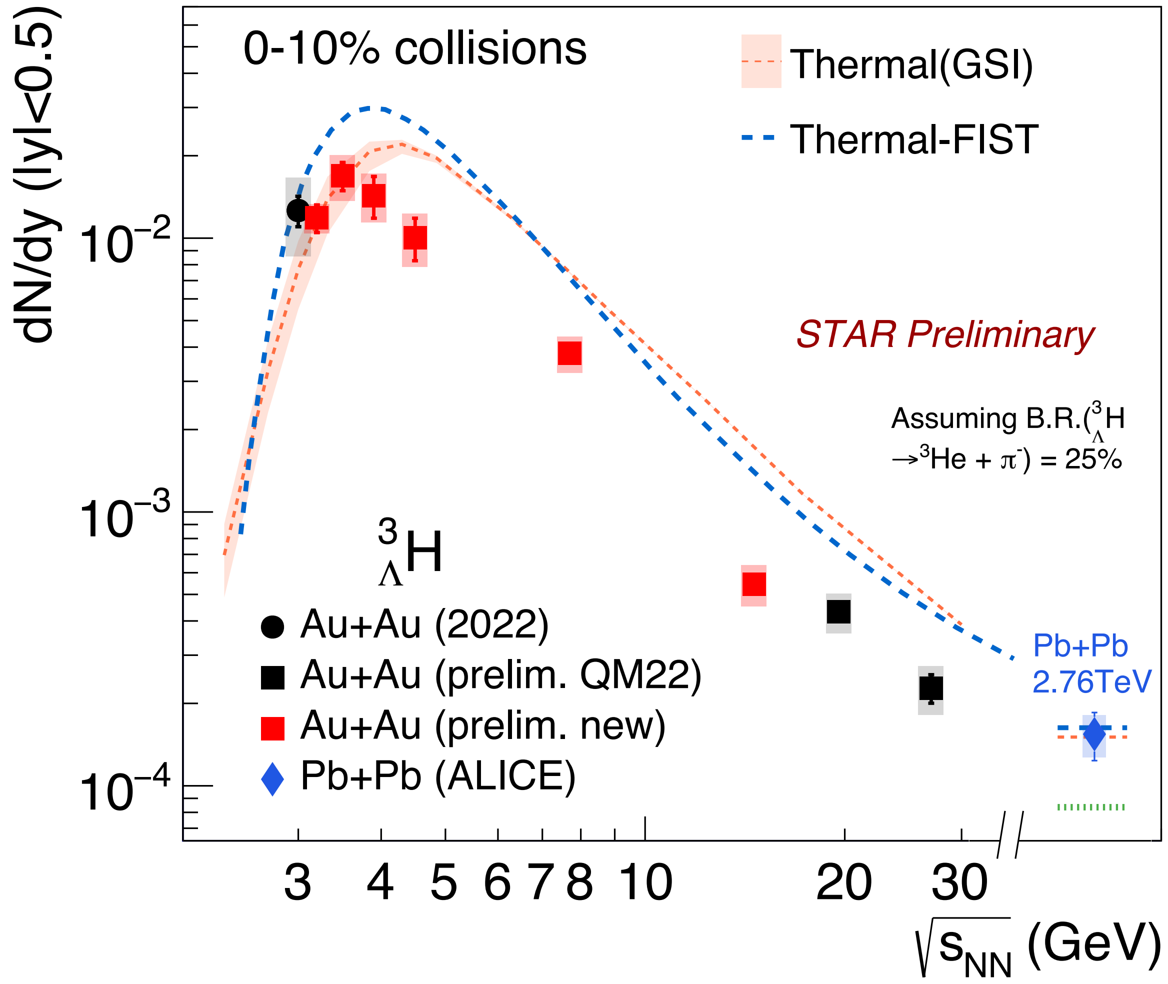

Thermal model

Hadron chemical freeze-out T_{ch} and μ_B.

Both hypertriton and triton yields are not fixed at chemical freeze-out (disfavor thermal)

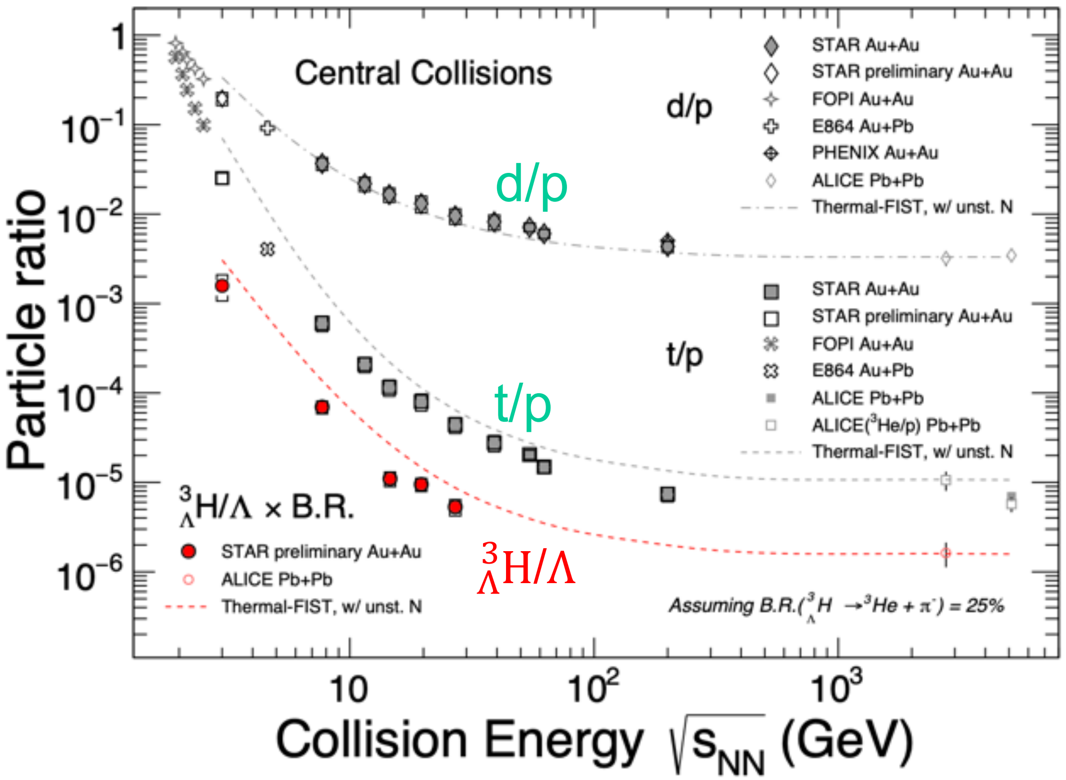

Thermal (GSI): A. Andronic et al. PLB 697,203-207 (2011)
Thermal-FIST, Coal. (UrQMD): T. Reichert et al. PRC 107 (2023) 1, 014912

Hypernuclei Yield vs. $\sqrt{s_{NN}}$

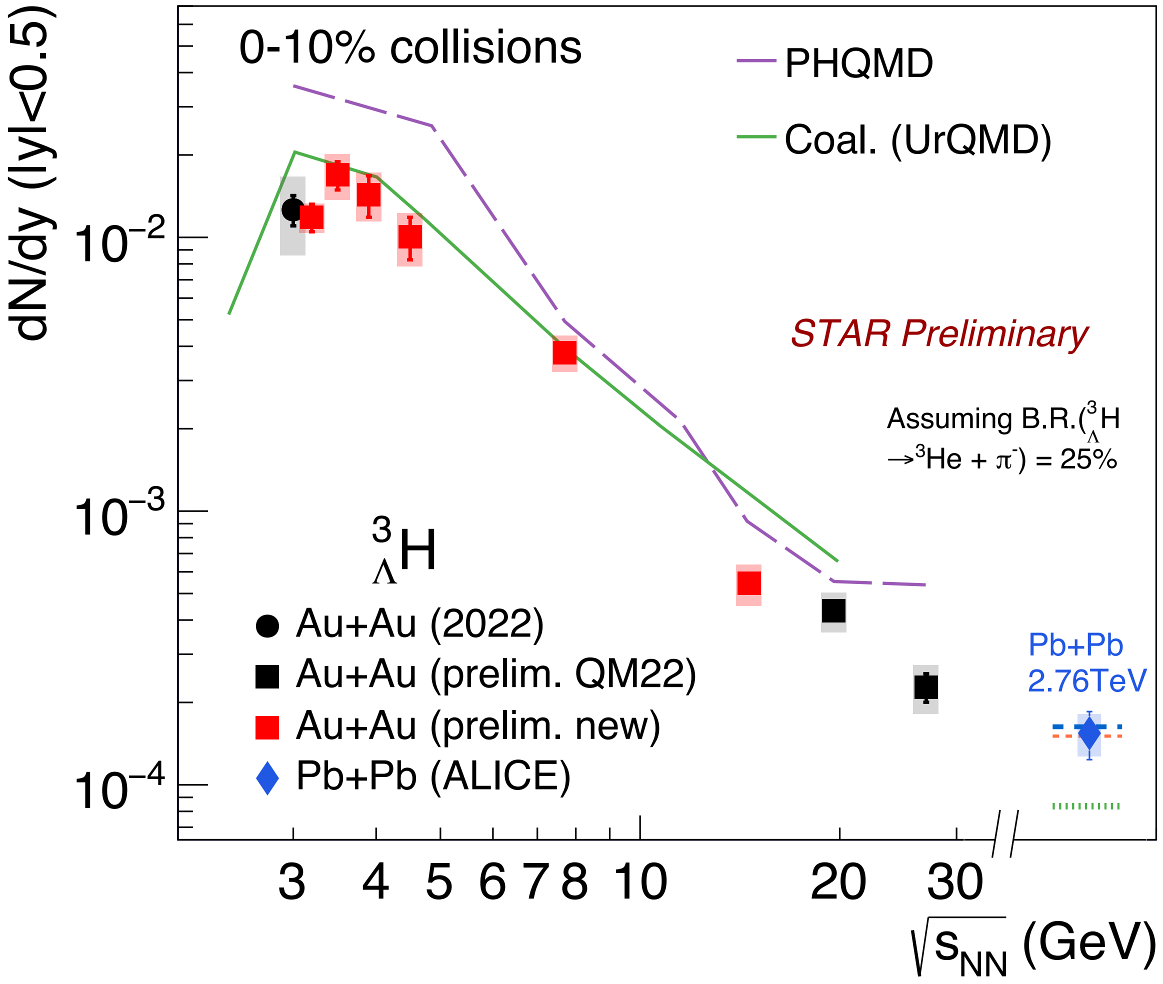

UrQMD + Coal.

Instant coalescence after hadron kinetic freeze-out.

Coalescence condition:

- $|\vec{p_1} - \vec{p_2}| < \Delta P, \quad |\vec{r_1} - \vec{r_2}| < \Delta R$

or Wigner Coalescence

PHQMD

Transport model + dynamical cluster formation.

Cluster can be formed before hadron kinetic freeze out.

Assuming

Y-N potential = 2/3 N-N potential.

Provide first constraints for hypernuclelproduction models in the high-baryon-densityregion

Coal. (UrQMD): T. Reichert et al. PRC 107 (2023) 1, 014912

PHQMD: S. Gläßel et al. PRC 105, 014908 (2022), V. Kireyeu et al. arXiv:1911.09496

Hypernuclei to Nuclei Ratios

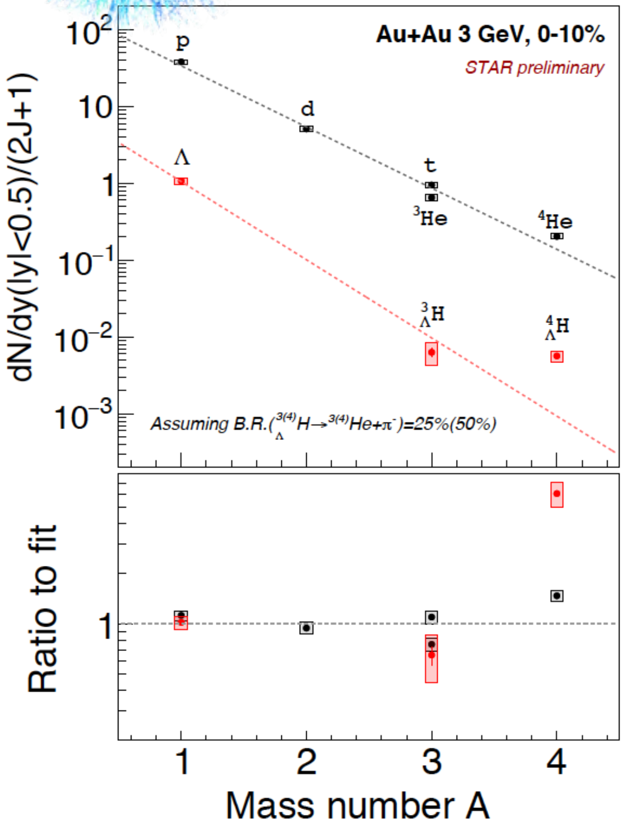

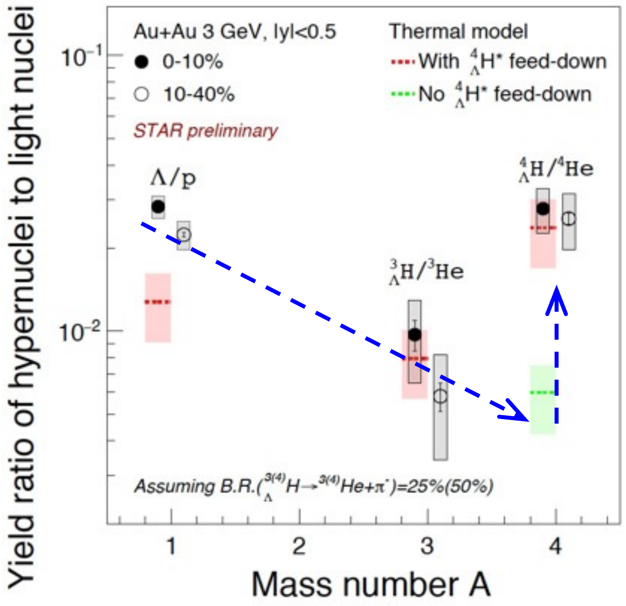

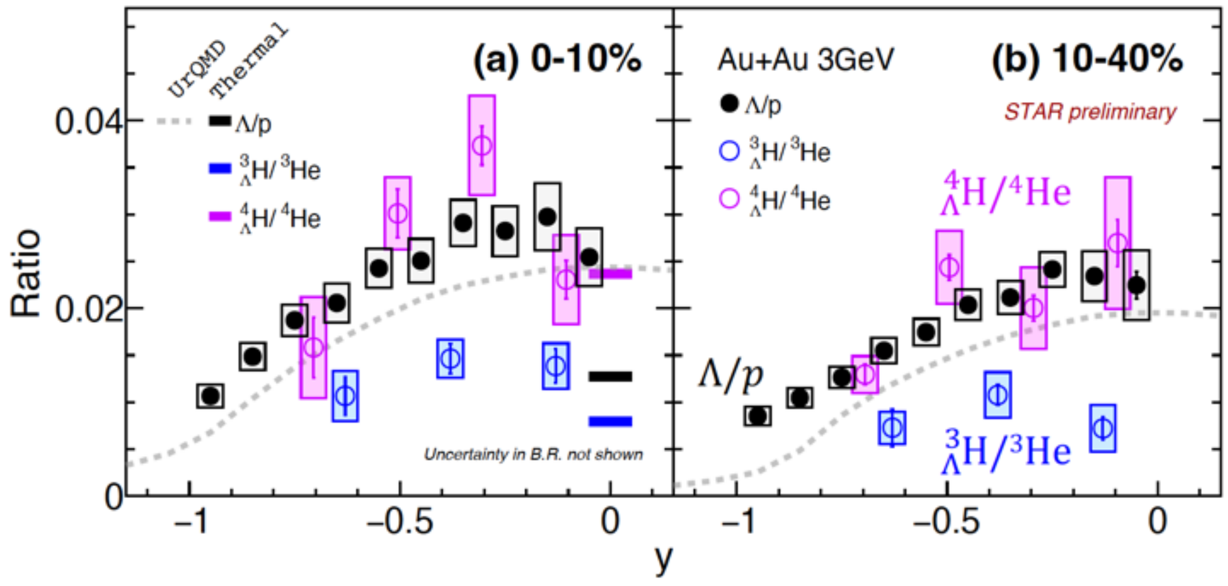

- $^{3}_{\Lambda}H/He^{3}$ yield ratios is lower than to that of Λ/p at both 0-10% and 10-40% centrality
  $^{4}_{\Lambda}H/He^{4}$ yield ratios are comparable to that of Λ/p in Au+Au collisions at 3 GeV.
- UrQMD model with coalescence describes the tendency of the distributions reasonably

- Enhanced $^{4}_{\Lambda}H$ production indicates a significant excited state feed-down contributions.

$$^{4}_{\Lambda}H^{*}(J^{+}=1) \rightarrow {}^{4}_{\Lambda}H^{*}(J^{+}=0) + \gamma$$

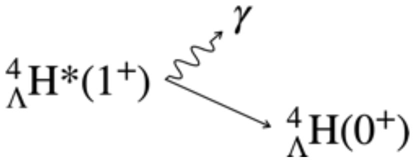

Suggest coalescence mechanism and creation of excited A = 4 hypernuclei

Strangeness Population Factor @ 3GeV

Phys. Lett. B 684 (2010) 224,
Phys. Rev. C 99, 054905 (2019)

- Connection to coalescence parameters

$$S_A = \frac{{}^{A}_{\Lambda}\mathrm{H}(A \times p_T)}{{}^{A}\mathrm{He}(A \times p_T) \times \frac{\Lambda}{p}(p_T)} = \frac{B_A({}^{A}_{\Lambda}\mathrm{H})(p_T)}{B_A({}^{A}\mathrm{He})(p_T)}$$

$$E_A \frac{d^3 N_A}{dp_A^3} = B_A \left(E_{p,n} \frac{d^3 N_{p,n}}{dp_{p,n}^3} \right)^A \Bigg|_{\vec{p}_p = \vec{p}_n = \frac{\vec{p}_A}{A}}$$

Under some coalescence scenarios:

$$B_A = \frac{2J_A + 1}{2^A} \frac{1}{\sqrt{A}} \frac{1}{m_T^{A-1}} \left(\frac{2\pi}{R^2 + (\frac{r_A}{2})^2} \right)^{\frac{3}{2}(A-1)}$$

Source size Radius

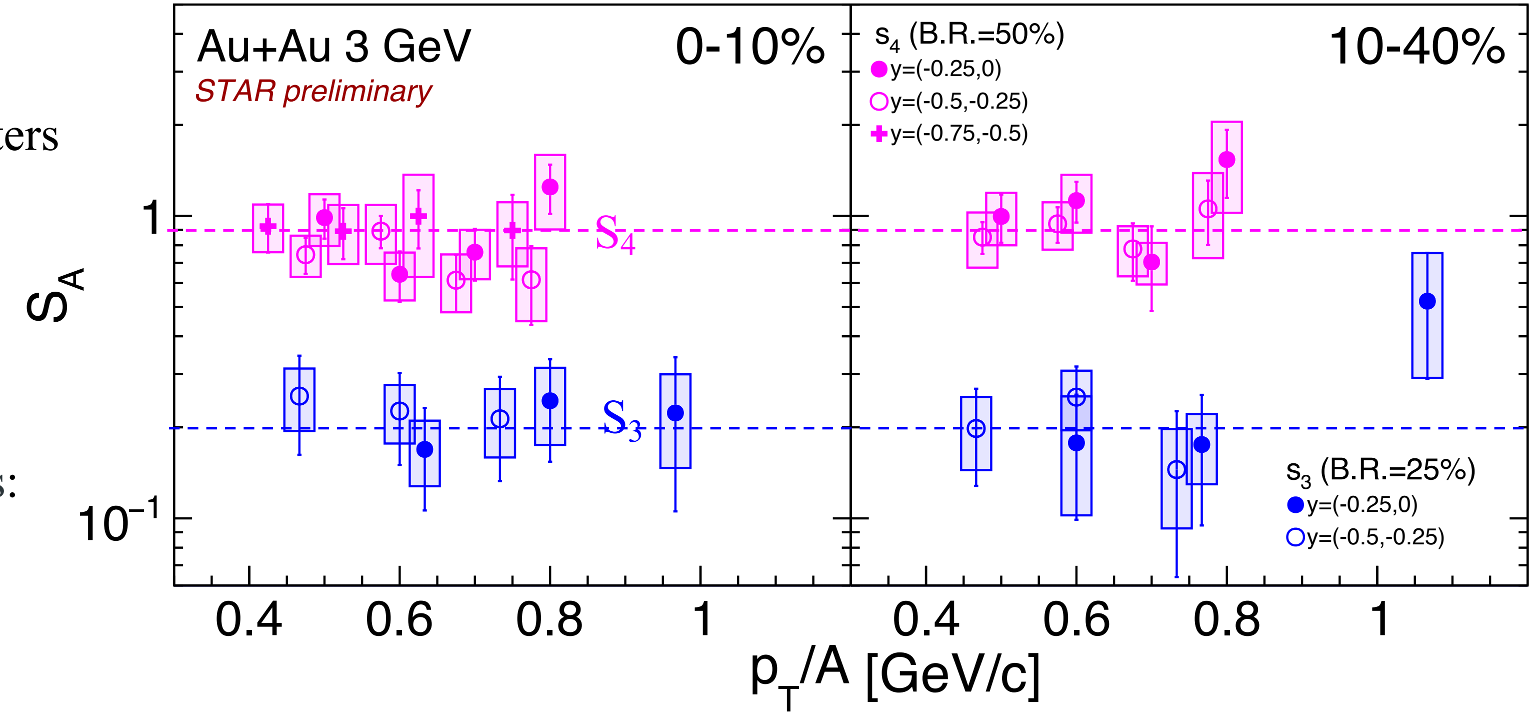

- S_A, direct connection to coalescence parameters. Which can be used to set additional constrains on hypertriton structure, radius and source size.
- No obvious p_T, rapidity and centrality dependence of S_A observed at 3 GeV.
- Evidence that B_A of light and hyper nuclei follow similar tendency, mechanics behind formation for hypernuclei and nuclei are similar

Strangeness Population Factor vs. $\sqrt{s_{NN}}$

Increasing trend of S_3 originally proposed as a signature of onset of deconfinement

$$S_3 = \frac{{}^{3}_{\Lambda}H}{{}^{3}He \times \frac{\Lambda}{p}}$$

: removes the absolute difference of Λ/B yields versus beam energy.

- Data shows a hint of an increasing trend

- Coalescence + transport also suggest increasing trend – the energy dependence is sensitive to the source size, ${}^{3}_{\Lambda}H$ suppression due to large size *Phys. Rev. C 107 (2023) 1, 014912* *Phys. Let. B 809 (2020) 135746*

- Thermal-FIST also suggest increasing trend : unstable nuclei breakup ${}^{4}Li \rightarrow {}^{3}He\, p$

$$S_2 = \frac{{}^{3}_{\Lambda}H}{\Lambda \times d}$$

: recently s_2 also proposed as a sensitive probe *Chin. Phys. C 44, 11 (2020) 114001*

Phys. Lett. B 684 (2010) 224

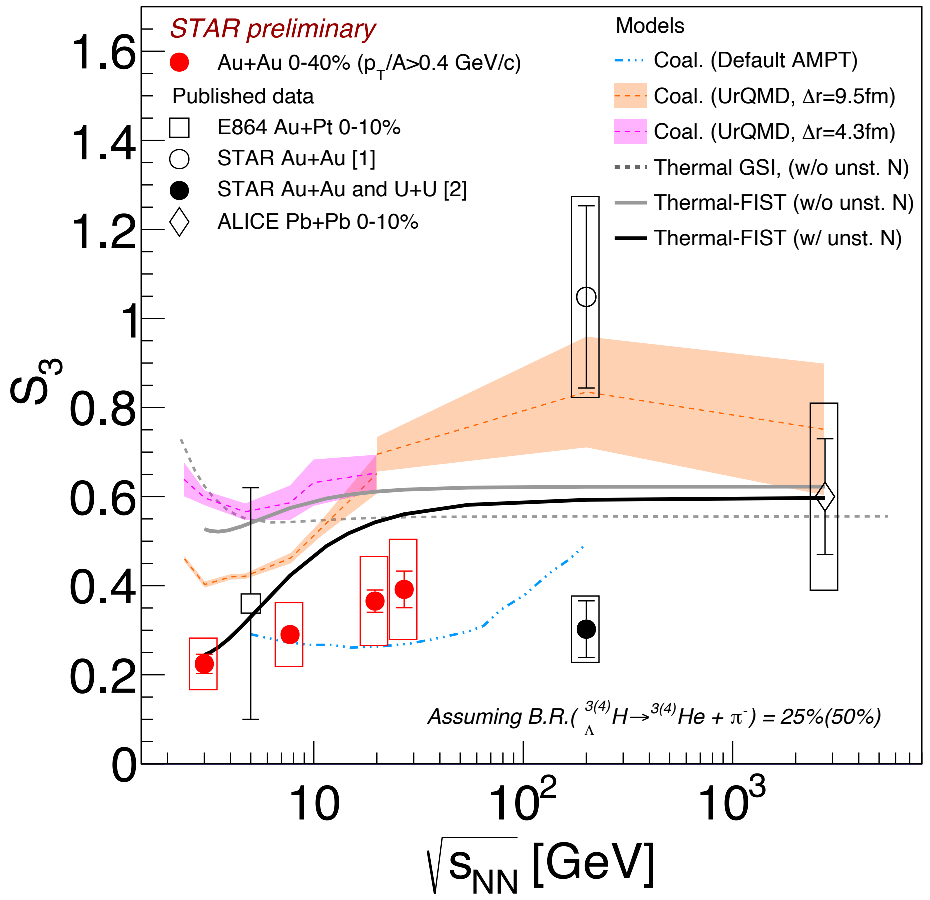

Provide constraints for hypernuclei production models in the high-baryon-density region

Note: For 19.6 and 27 GeV, take ${}^{3}He/t = 0.93 \pm 0.07$

Summary

- HyperNuclei Measurements @ STAR
  - ✓ Intrinsic Properties:
    -- Lifetime, Branch Ratios & Binding Energy
  - ✓ Productions and Collectivity:
    -- Centrality, Rapidity & Energy Dependence

- ✓ Enhanced hypernuclei production at low energies allow precision measurement
- ✓ STAR data support coalescence mechanism of hypernuclei formation at mid-rapidity
- ✓ Hypernuclei are not in equilibrium at hadron chemical freeze-out at RHIC energies

Outlook

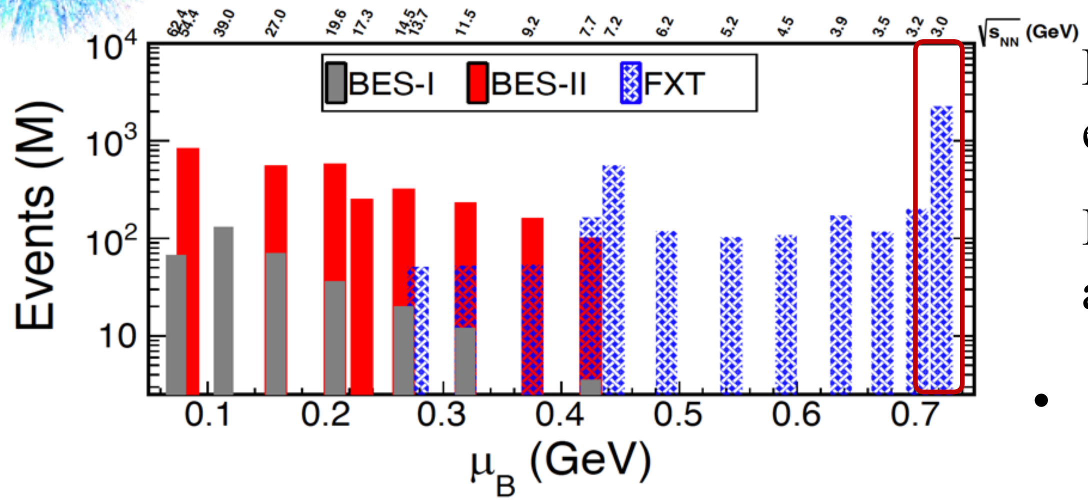

High statistical data from BES-II and other facilities and experiments

In this report: Part of the STAR BES-II dataset are analyzed and reported, stay tune

- Systematic and precise measurements of the hypernuclei production and the properties, ${}^3_\Lambda H, {}^4_\Lambda H, {}^4_\Lambda He, {}^5_\Lambda He$,etc: Y-N, YY, EoS

${}^A_\Lambda$H/Λ vs energy

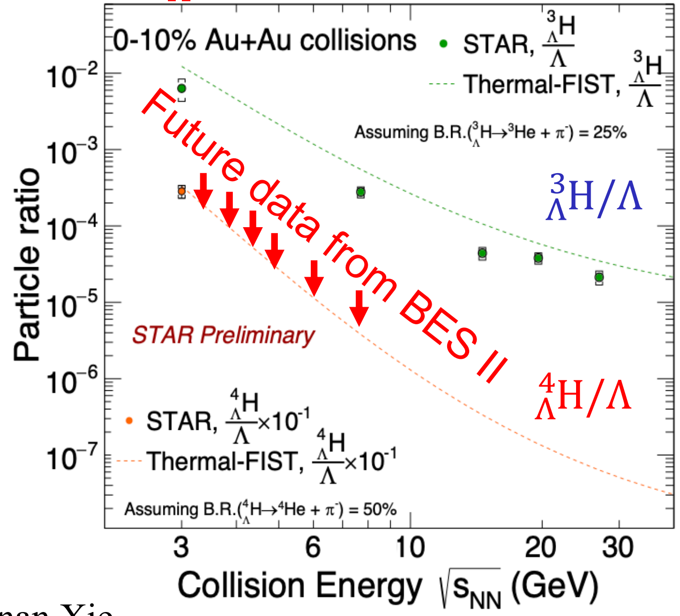

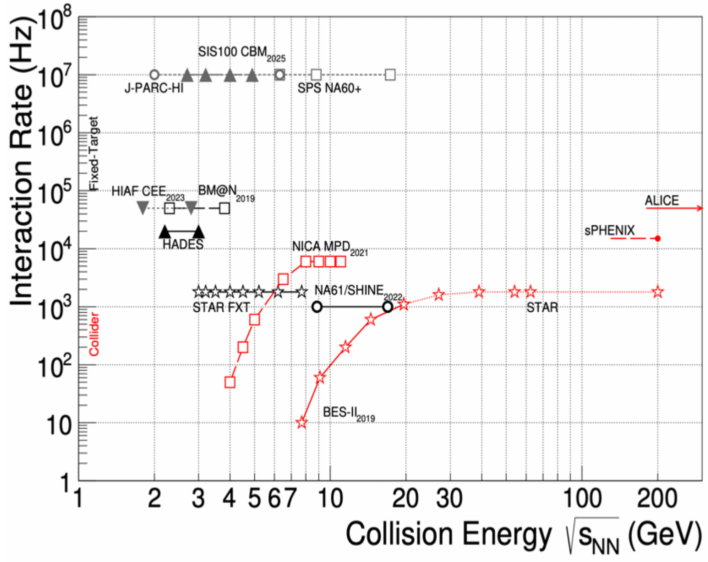

- Double Λ hypernuclei (YY) ${}^4_{\Lambda\Lambda}$H-> ${}^4_\Lambda$Heπ, ${}^5_{\Lambda\Lambda}$H -> ${}^5_\Lambda$Heπ
- Particle correlations $p-\Lambda, d-\Lambda, \Lambda-\Lambda$ correlations.

中国科学院大学
University of Chinese Academy of Sciences
Thanks for Listening!

Directed Flow (v_1) and $<p_T>$ at 3 GeV

PRL 130 (2023) 212301

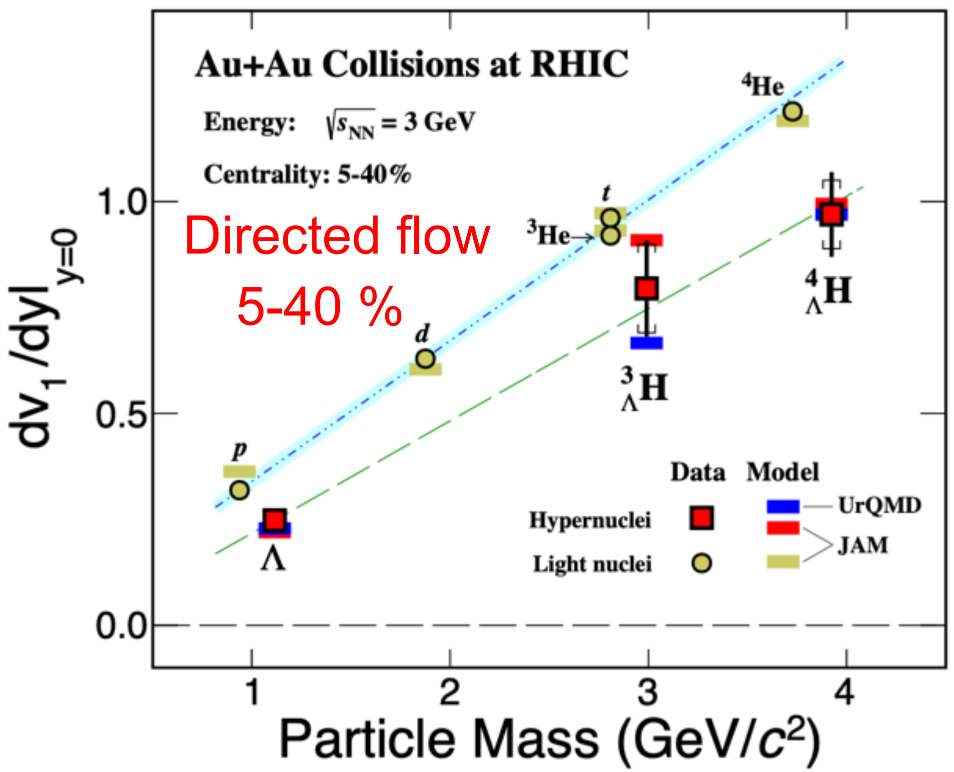

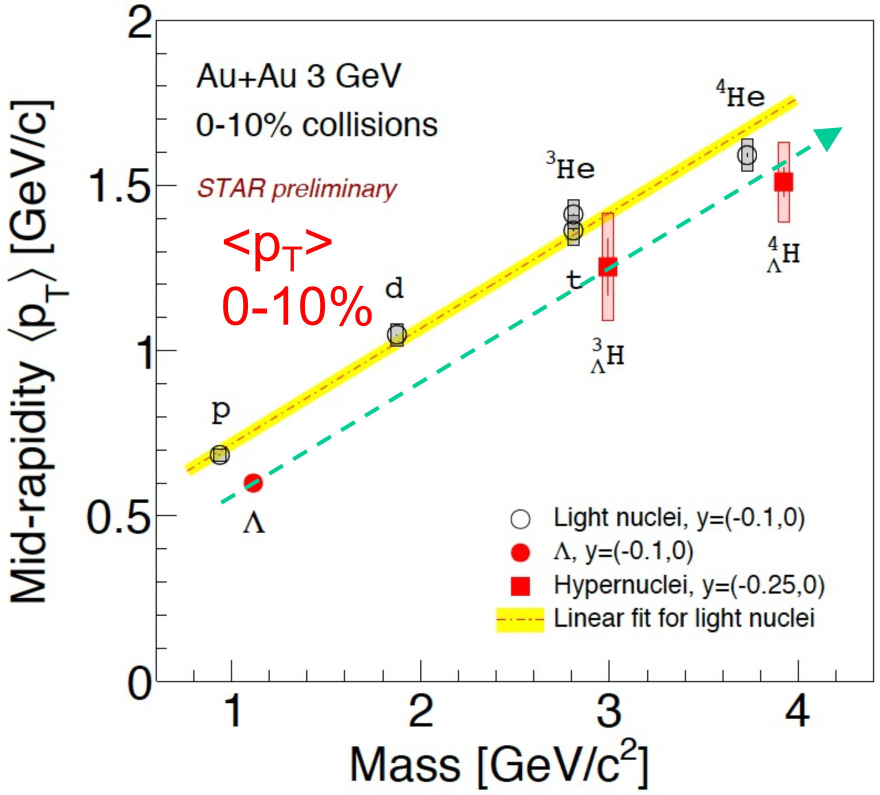

- v_1 slope following mass number scaling.

$$E\frac{d^3N}{dp^3} = \frac{1}{2\pi}\frac{d^2N}{p_T dp_T dy}\left(1 + \sum_{1}^{\infty} 2v_n \cos\left[n\left(\phi - \psi_{RP}\right)\right]\right)$$

- Similar phenomena also seen in $<p_T>$.
 - Radial flow contribution.

Mid-rapidity results qualitatively consistent with that the hypernuclei production is from coalescence of hyperons and nucleons.

Strangeness Population Factor

Small emitting source 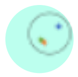 Large emitting source 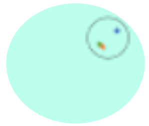

S. Zhang et al, PLB 684, 224 (2010)

$$S_A = \frac{{}^{A}_{\Lambda}\mathrm{H}(\mathrm{A}\times \mathrm{p_T})}{{}^{A}\mathrm{He}(\mathrm{A}\times \mathrm{p_T})\times \frac{\Lambda}{\mathrm{p}}(\mathrm{p_T})} = \frac{\mathrm{B_A}({}^{A}_{\Lambda}\mathrm{H})(\mathrm{p_T})}{\mathrm{B_A}({}^{A}\mathrm{He})(\mathrm{p_T})}$$

$$E_A \frac{d^3 N_A}{dp_A^3} = B_A \left(E_{\mathrm{p,n}} \frac{d^3 N_{\mathrm{p,n}}}{dp_{\mathrm{p,n}}^3} \right)^A \Bigg|_{\vec{p}_{\mathrm{p}}=\vec{p}_{\mathrm{n}}=\frac{\vec{p}_A}{A}}$$

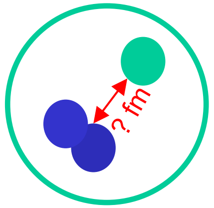

Under some coalescence scenarios:

PRC 99, 054905 (2019)

$$B_A = \frac{2J_A+1}{2^A}\frac{1}{\sqrt{A}}\frac{1}{m_T^{A-1}}\left(\frac{2\pi}{R^2+(\frac{r_A}{2})^2}\right)^{\frac{3}{2}(A-1)}$$

Source size Radius

- Direct connection to coalescence parameters.
- Larger radius would have stronger source size dependence.
- Additional constrains on hypertriton structure.

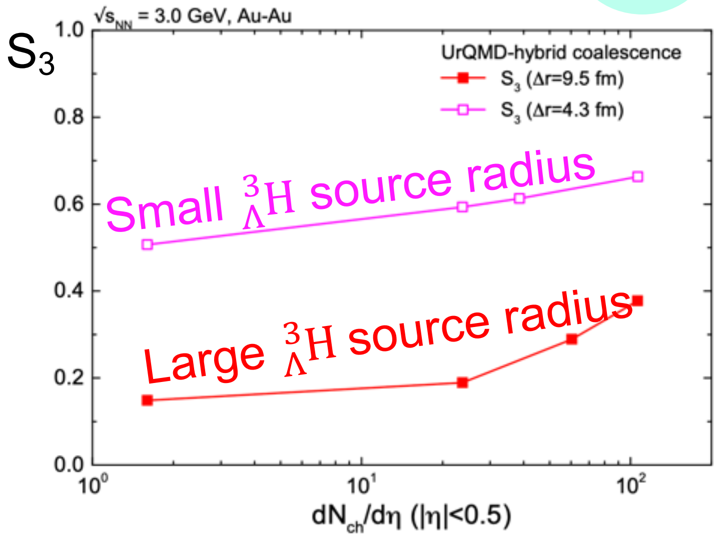

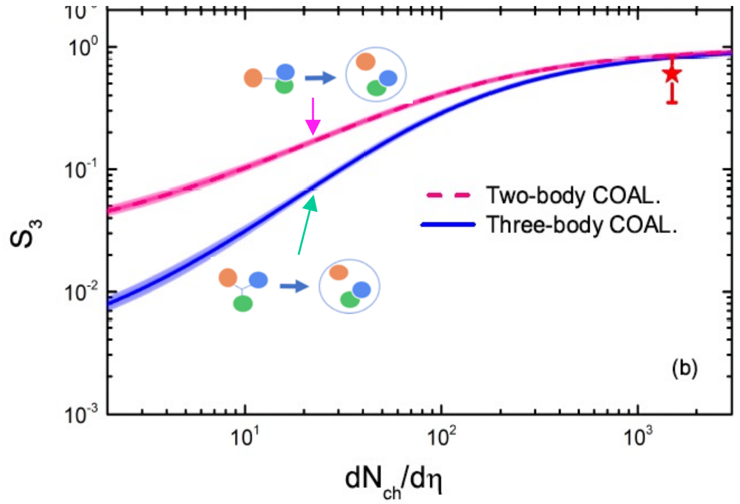

Phys. Rev. C 107, 014912 (2023)

Phys. Lett. B 792 (2019) 132-137

Hypertriton Branching Ratio

- Model comparison show data favors small B_{Λ}, weakly bounded state of ${}^{3}_{\Lambda}H$
- Stronger constraints on absolute B.R. and hypertriton internal structure models

$$R_3 = \frac{B.R.({}^{3}_{\Lambda}H \rightarrow {}^{3}He\,\pi^-)}{B.R.({}^{3}_{\Lambda}H \rightarrow p\,d\,\pi^-) + B.R.({}^{3}_{\Lambda}H \rightarrow {}^{3}He\,\pi^-)}$$

STAR: $R_3 = 0.272 \pm 0.030 \pm 0.042$

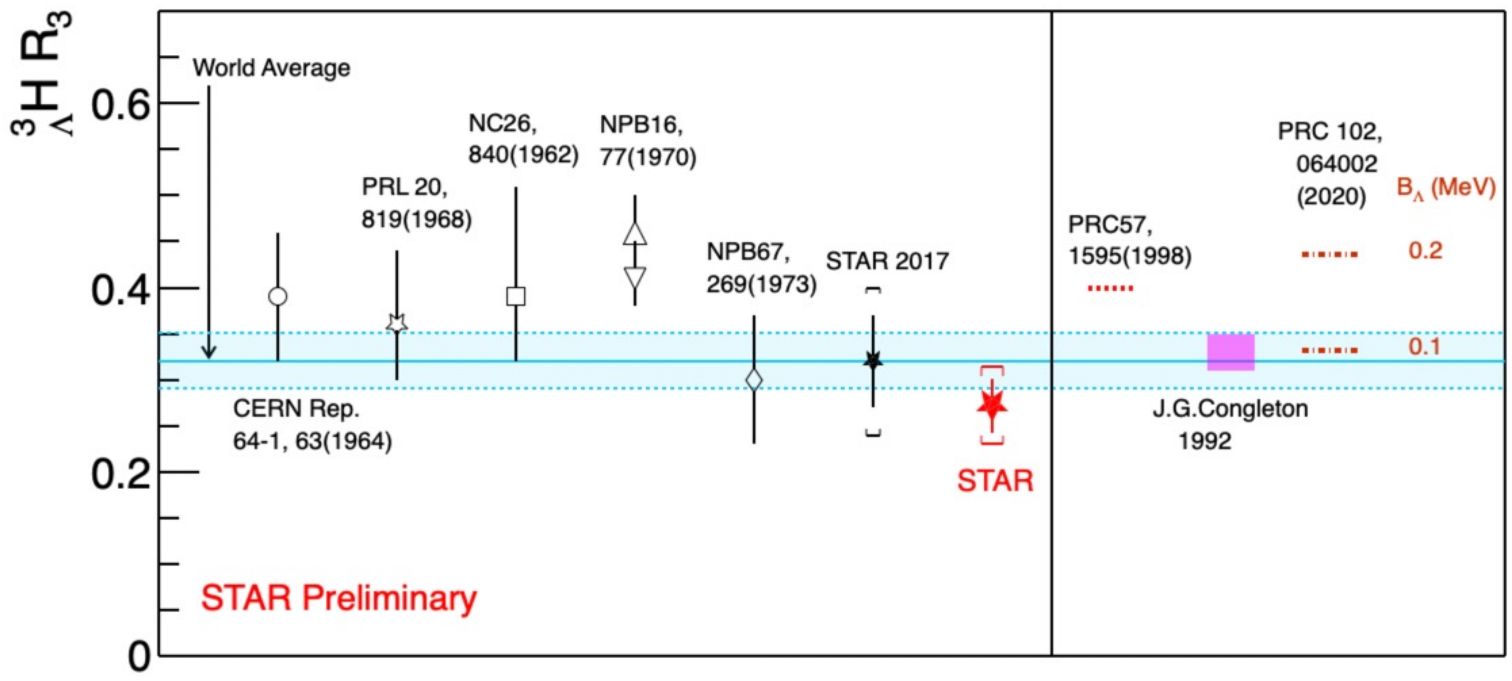

$B_{\Lambda} = (m_d + m_{\Lambda} - m_{{}^{3}_{\Lambda}H})$